

CHAPTER III

COMPLEXING BEHAVIOUR OF (E)-4-(4-METHOXYBENZYLIDENEAMINO)-6-METHYL-3-THIOXO-3,4-DIHYDRO-1,2,4-TRIAZIN-5(2H)-ONE (MMTDT), (E)-4-(2-CHLOROBENZYLIDENEAMINO)-6-METHYL-3-THIOXO-3,4-DIHYDRO-1,2,4-TRIAZIN-5(2H)-ONE (CBMTDT) AND (E)-4-(1-(2-HYDROXYPHENYL)ETHYLIDENEAMINO)-6-METHYL-3-THIOXO-3,4-DIHYDRO-1,2,4-TRIAZIN-5(2H)-ONE (HEMTDT).

- 3.1 REVIEW OF LITERATURE
- 3.2 SYNTHESIS OF MMTDT, CBMTDT AND HEMTDT
- 3.3 PREPARATION OF METAL COMPLEXES OF MMTDT, CBMTDT AND HEMTDT
- 3.4 PHYSICAL MEASUREMENTS
- 3.5 COMPUTATIONAL STUDIES
- 3.6 MOLECULAR MODELING STUDIES
- 3.7 RESULTS AND DISCUSSION
- 3.8 CONCLUSION
- 3.9 REFERENCES

Part of the work presented in this chapter is communicated to Journal of coordination chemistry.GCOO-2011-0300 (Revision submitted).

3.1 REVIEW OF LITERATURE

6-substituted -4-amino-5-mercapto-1, 2, 4-triazines are sulfur and nitrogen donor ligands and are potentially multidentate in nature. The prominent coordination sites are i) sulfur of mercapto group, ii) nitrogen of primary and secondary groups and iii) two nitrogen atoms at positions 1 and 2 in the triazine ring system. It is generally established that bidentate or multidentate ligands, in common, form more complexes than monodentate ligands.

The triazine ligands contain both 'hard' nitrogen and 'soft' sulfur as donor atoms. It will be interesting, therefore to investigate the nature of bonding with metal ions in these ligands because metal ions of 'class a' group have preference for coordination with hard nitrogen and 'class b' group of metal ions have preference for coordination with soft sulfur. The study of organic ligands containing two or more different donor atoms have considerable interest because such ligands throw light on the nature of metal-sulfur bonding. Many quantitative studies have confirmed that metal chelates are more stable than those of related unidentate ligands. Besides, five or six membered chelates are by far the most common and are in general the most stable. It was shown that sulfur and nitrogen containing substituents increase the stability of complexes on account of chelate effect.

The substituted 1, 2, 4-triazines contain a thioamide moiety and naturally this group gives four characteristic thioamide bands. The study of systematic shifts in the position of these thioamide bands in the infrared spectra can give clues regarding the nature of metal- sulfur and metal- nitrogen bonding.

The growing interest in triazine derivatives stems from their potential application as agrochemicals. Recent studies have shown their ability in chelating transition metal ions to form stable complexes [1-2]. They provided wide range of applications in the field of optics, herbicides and pharmaceuticals as well [3-6]. Triazine based herbicides have gained world wide recognition. The major problems experienced due to herbicides are the contamination of soil, surface water, and possibly ground water with their residuals. Systematic study of residual substituted triazine and related

compounds are necessary [7-9]. Studies have therefore needed to evaluate the toxicities of several substituted triazine and their metal complexes in order to understand the role of substituent and metal complexation in modifying the activities of s-triazine herbicides [10].

Numerous compounds containing 1, 2, 4-triazine moiety [11-12] is well known in natural products and show interesting biological and antiviral properties. Many derivatives of 1, 2, 4-triazine compounds form colored complexes with different metal ions and can be used as analytical reagent for their determination. Schiff bases containing different donor atoms also find use as corrosion inhibitors as they are selective and sensitive towards various metal ions [13-15]. 1, 2, 4-triazines are known to be biologically active: they act as antiviral, antibacterial, antimalarial and anti-inflammatory agents [16-19]. Their anticancer, antileukemia and anti HIV activities have been evaluated and found to be promising in some instances [20-23].

G.Singh et al. reported certain polymeric complexes of Co(II),Ni(II), Cu(II) and Zn(II) in 1:1 and 1:2 molar ratio with schiff bases derived from the condensation of 4-amino-3-mercapto-6-methyl-5-oxo-1,2,4-s-triazine with anisaldehyde ,indole-3-carboxaldehyde, acetophenone and o-vanillin. The ligand act as bidentate S, N donor in the first three cases and as terdentate S, N, O donor in the last case [24]. B.Kebede et al. reported the synthesis and characterization of s-triazine herbicide,2,4,6-tris(hydrazine)-s-triazine and its Co(II),Ni(II),Cu(II) and Zn(II) complexes. Ring nitrogen as well as terminal nitrogen of hydrazine side chain was proposed as metal binding centres [10].

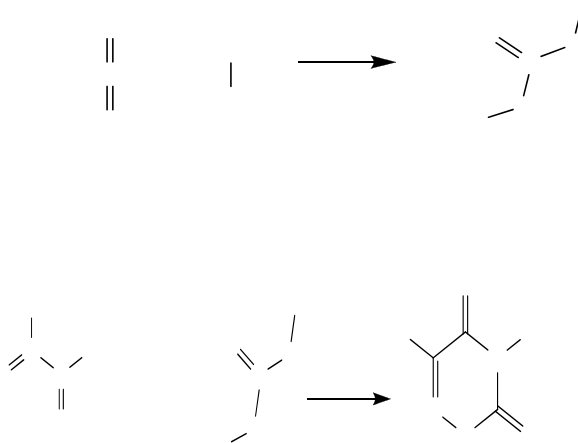
K.Singh et al. also reported polynuclear complexes of Co(II),Ni(II),Cu(II) and Zn(II) with schiff base derived from the condensation of 4-amino-3-mercapto-6-methyl-5-oxo-1,2,4 -triazine with 2-acetyl pyridine. The ligand coordinates through nitrogen and sulfur atoms. They also conducted some antibacterial studies by using MIC method [25]. S.S.Kandil synthesized a series of Co(II),Co(III) and Cu(II) complexes of 3-(2-furylidene) hydrazine-5,6-diphenyl-1,2,4-triazine. Spectral studies suggest that ligand act as bidentate towards divalent metal ions through a triazine-N, and azomethine-

N, and act as tridentate towards Co(III) via same two nitrogen atoms and the furan-Oxygen [26].

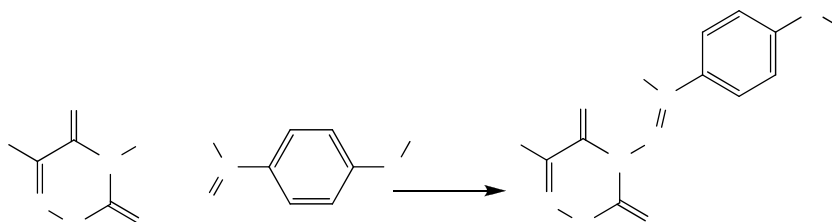
K.Mamatha et al. reported synthesis and characterization of Co(II), Ni(II), Cu(II), Zn(II), Pd(II) and Cd(II) complexes of schiff base derived from 3-amino-2-mercaptoquinazoline-4(3H)-one and pyridine 2-carboxaldehyde, thiophene 2-carboxaldehyde & 3-formylchromone. The ligand act as a bidentate one, coordinating through quinazoline carbonyl oxygen and azomethine nitrogen [27].

3.2 SYNTHESIS OF MMTDT, CBMTDT AND HEMTDT

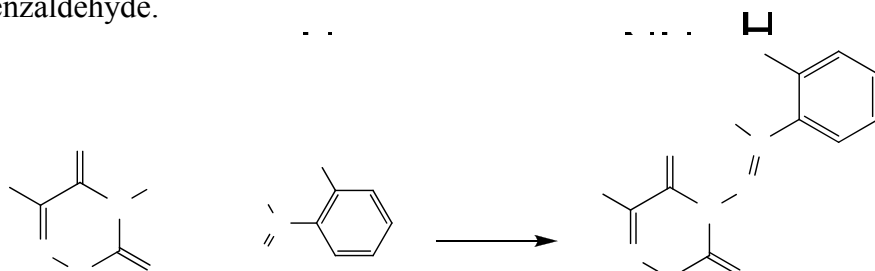
These ligands were synthesized in three stages. In the first stage, Carbon disulphide on reaction with hydrazine hydrate produces thiocarbohydrazide which on reaction with 2-oxopropionic acid produces 4-amino-6-methyl-3-thioxo-3,4-dihydro-1,2,4-triazin-5(2H)-one (2nd stage) [28-29].



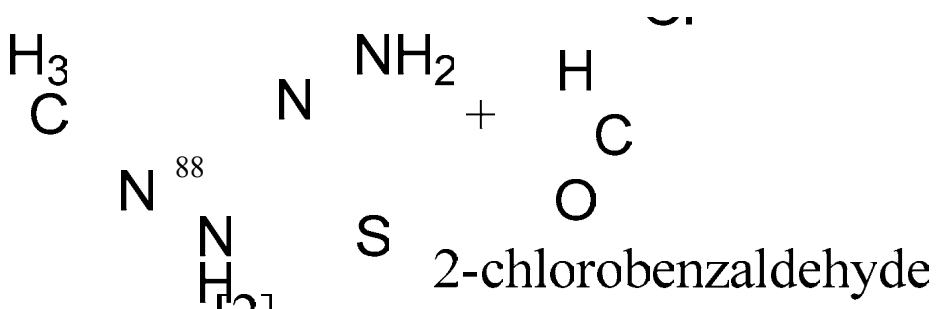
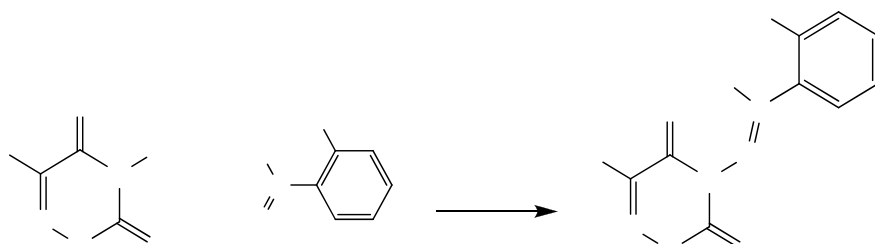
a. (E)-4-(4-methoxybenzylideneamino)-6-methyl-3-thioxo-3, 4-dihydro-1, 2, 4-triazin-5(2H)-one (MMTDT) is synthesised by condensation of 4-amino-6-methyl-3-thioxo-3, 4-dihydro-1, 2, 4-triazin-5(2H)-one with 4-methoxybenzaldehyde.



b. (E)-4-(2-chlorobenzylideneamino)-6-methyl-3-thioxo-3,4-dihydro-1,2,4-triazin-5(2H)-one (CBMTDT) was synthesised by condensation of 4-amino-6-methyl-3-thioxo-3,4-dihydro-1,2,4-triazin-5(2H)-one with 2-chlorobenzaldehyde.



c. (E)-4-(2-hydroxyphenyl) ethylideneamino)-6-methyl-3-thioxo-3,4-dihydro-1,2,4-triazin-5(2H)-one (HEMTDT) was synthesised by condensation of 4-amino-6-methyl-3-thioxo-3,4-dihydro-1,2,4-triazin-5(2H)-one with 2-hydroxybenzaldehyde.



3.3 PREPARATION OF METAL COMPLEXES OF MMTDT, CBMTDT AND HEMTDT

3.3.1 [Diaquobis[(E)-4-(4-methoxybenzylideneamino)/(E)-4-(2-chlorobenzylideneamino)/ (E)-4-(2-hydroxyphenyl) ethylideneamino)]-6-methyl-3-thioxo-3, 4-dihydro-1, 2, 4-triazin-5(2H)-one] cobalt(II)

To a hot solution of cobalt acetate (0.01 M) in water, a hot ethanolic solution of MMTDT/CBMTDT/HEMTDT (0.02 M) was added drop wisely .The mixture was shaken well and refluxed for 5 hours. The resulting solution was cooled, filtered and washed with water, ethanol and dried. The obtained reddish brown coloured complex is soluble in DMSO.

3.3.2 [Diaquobis [(E)-4-(4-methoxybenzylideneamino) / (E)-4-(2-chlorobenzylideneamino)/ (E)-4-(2-hydroxyphenyl) ethylideneamino)] 6-methyl-3-thioxo-3, 4-dihydro-1, 2, 4-triazin-5(2H)-one] nickel(II)

The complex was prepared by adding hot ethanolic solution of MMTDT/CBMTDT/HEMTDT (0.02M) to aqueous solution of nickel acetate (0.01 M).The mixture was refluxed for 3-5 hours .The dark green coloured complex formed was cooled, filtered, washed and dried. The solid obtained is soluble in DMSO.

3.3.3 [Diaquobis [(E)-4-(4-methoxybenzylideneamino)/(E)-4-(2- chlorobenzylideneamino)/ (E)-4-(2-hydroxyphenyl) ethylideneamino)]-6-methyl-3-thioxo-3, 4-dihydro-1, 2, 4-triazin-5(2H)-one] platinum(IV) chloride

To the hot aqueous solution of Chloroplatinic acid (0.01M), hot ethanolic solution of MMTDT/CBMTDT/HEMTDT (0.02 M) is added dropwisely, shaken well and refluxed for 5 hours. The dark brown coloured solution obtained was cooled, washed and dried at 100⁰C.The resulting solid is soluble in DMSO and DMF.

3.3.4 [bis [(E)-4-(4-methoxybenzylideneamino)/(E)-4-(2-chlorobenzylideneamino)/ (E)-4-(2-hydroxyphenyl) ethylideneamino)]-6-methyl-3-thioxo-3, 4-dihydro-1, 2, 4-triazin-5(2H)-one] copper(II)

Copper complex is prepared by adding hot ethanolic solution of 0.02M MMTDT/CBMTDT/HEMTDT to aqueous solution of 0.01M copper acetate solution and refluxed for 5 hours. The resulting solution was cooled, filtered, washed and dried. The brown coloured solid obtained is soluble in DMSO and is characterized by various analytical and spectral studies.

3.3.5 bis[(E)-4-(4-methoxybenzylideneamino)/(E)-4-(2-chlorobenzylideneamino)/ (E)-4-(2-hydroxyphenyl) ethylideneamino)]-6-methyl-3-thioxo-3, 4-dihydro-1, 2, 4-triazin-5(2H)-one] zinc(II)

The complex was prepared by the procedure given in 2.4.5 by using zinc acetate. The dried complex is yellow in colour.

3.3.6 [Diaquobis [(E)-4-(4-methoxybenzylideneamino)/(E)-4-(2-chlorobenzylideneamino)/ (E)-4-(2-hydroxyphenyl) ethylideneamino)]-6 methyl-3-thioxo-3, 4-dihydro-1, 2, 4-triazin-5(2H)-one] cadmium(II)

Cadmium complex was prepared by refluxing 0.01M aqueous solution of cadmium acetate and 0.02M ethanolic solution of MMTDT/CBMTDT/HEMTDT for 5 hours. The resulting dark yellow coloured complex was cooled, filtered, washed and dried.

3.3.7 [Diaquobis [(E)-4-(4-methoxybenzylideneamino)/(E)-4-(2-chlorobenzylideneamino)/ (E)-4-(2-hydroxyphenyl) ethylideneamino)]-6-methyl-3-thioxo-3, 4-dihydro-1, 2, 4-triazin-5(2H)-one] mercury(II)

To a hot ethanolic solution of MMTDT/CBMTDT/HEMTDT (0.02 M), aqueous solution of 0.01M mercuric acetate added and refluxed for 4-5 hours. The resulting black coloured complex was cooled, filtered, washed and dried.

3.3.8 [Diaquobis [(E)-4-(4-methoxybenzylideneamino)/(E)-4-(2-chlorobenzylideneamino)/(E)-4-(2-hydroxyphenyl)ethylideneamino)]-6-methyl-3-thioxo-3,4-dihydro-1,2,4-triazin-5(2H)-one] palladium (II)

The complex was prepared by the procedure given in 2.4.7 by using palladium chloride. The dried complex was brown in colour and is soluble in DMSO.

3.4 PHYSICAL MEASUREMENTS

Elemental analyses were carried out on an Elementar Vario EL III model elemental analyzer at STIC, CUSAT, Cochi. ¹H NMR spectra were recorded using a model Bruker GmbH DPX-300 MHz FT spectrometer using DMSO as solvent. Absorption spectrophotometric studies (Jasco V-550) and infrared spectra (KBr/CsI) on a Jasco FT/IR-4100 spectrophotometer were carried out in the department. Magnetic susceptibility measurements were carried out using the standard Gouy tube technique using Hg[Co(SCN)₄] as a calibrant in the department (Sherwood Scientific Cambridge, UK). Thermal analysis (TGA and DTA) were carried out in air atmosphere with a heating rate of 15 °C/min using Setaram made Labsys TGA-DTA 1600 system in the department and also at STIC Cochi. The ESR spectrum of the copper complex was recorded on a Varian E -112 spectrometer using TCNE as the standard at STIC, IIT, Mumbai.

3.5 COMPUTATIONAL STUDIES

The chemical reactivity of different sites of the ligand molecule was evaluated by Fukui indices defined by:

For nucleophilic attack

$$f_k^+ = q_{k(N+1)} - q_{k(N)}$$

For electrophilic attack

$$f_k^- = q_{k(N)} - q_{k(N-1)}$$

where $q_{k(N)}$, $q_{k(N-1)}$ and $q_{k(N+1)}$ are the electronic population of the atom k in neutral, cationic and anionic systems, respectively [30-31]. The condensed Fukui function is local reactivity descriptor and can be used only for comparing reactive atomic centers within the same molecule. Condensed softness indices allowing the comparison of reactivity between similar atoms of different molecules can be calculated easily starting from the relation between the Fukui function $f(r)$ and the local softness $S(r)$.

$$S(r) = (\partial \rho(r) / \partial N)_{v(r)} (\partial N / \partial \mu)_{v(r)} = f(r) S$$

All calculations, including geometry optimizations of the ligand molecule was performed with the B3LYP exchange correlation corrected functional with the 6-31G (d) basis set using the Gaussian 03W package. As shown by De Proft et al. [32-34], the B3LYP functional appears to be reliable for calculating $f(r)$ and f_k indices.

3.6 MOLECULAR MODELING STUDIES

The molecular geometry of the ligand and its complexes were first optimized at molecular mechanics (MM+) level. Semi empirical method PM3 is then used for optimizing the full geometry of the systems using Polak-Ribiere (conjugate gradient) algorithm and Unrestricted Hartree-Fock is employed keeping RMS gradient of $0.01 \text{ kcal}/(\text{mol} \text{ \AA}^0)$. All the parameters refer to isolated molecule in vacuum. All calculations were carried out by HyperChem 7.51 software package.

PreADMET is a web-based application for predicting ADME data and building drug like library using in silico method.

3.7 RESULTS AND DISCUSSION

The analytical and physical data of the three ligands and its complexes are given in Table III. 1A, 1B & 1C. This shows that all the used metal ions form ML_2 type complexes with MMTDT, CBMTDT and HEMTDT. The Co(II), Ni(II) and Pt(IV) complexes contain two molecules of water coordinated to the metal, which are confirmed by thermal and IR data.

3.7.1. Infrared Spectral Studies

The characteristic Infrared spectral bands of the ligand and its metal complexes are reported in Tables III. 2 A, 2B & 2C and the representative IR spectra are given in Fig.3.1A (i-iii), 1B (i-iii) & 1C (i-iii). All the synthesised complexes of MMTDT & CBMTDT ligand systems show the same trend. The following changes have been observed in the ligand after complexation.

MMTDT & CBMTDT complexes

The band at 1680 cm^{-1} ($\nu_{\text{C=O}}$) of the ligand is observed in the spectra of metal complexes also. This shows the non participation of the carbonyl group in bonding. A strong band at 1611 cm^{-1} in the free ligand was assigned to the azomethine group ($\nu_{\text{N=C-CH}_3}$) which shifts towards $\pm 10\text{-}20\text{ cm}^{-1}$ in the spectra of metal complexes indicating that coordination through nitrogen atom is due to the reduction of double bond character of carbon-nitrogen bond of the azomethine group [35-40]. Formation of metal-nitrogen bond is further supported by the appearance of a band in the region of $470\text{-}480\text{ cm}^{-1}$ in far IR spectra. The existence of thione form of the ligand has been proposed on the basis of a weak band observed for ($\nu_{\text{N-H}}$) around 3200 cm^{-1} and a strong band at $1135\text{-}1085\text{ cm}^{-1}$ due to ($\nu_{\text{C=S}}$). However, as expected, in the metal complexes a new band was observed at $750\text{-}760\text{ cm}^{-1}$ for ($\nu_{\text{C-S}}$). Metal-sulfur bond formation is further supported by the appearance of a band in the region $320\text{-}330\text{ cm}^{-1}$ in the far IR spectra [41]. Four characteristic thioamide bands are expected in the spectra of the ligand and the complexes. The position of the thioamide band I ($1530\text{-}1560\text{ cm}^{-1}$) in the spectrum of the ligand is not shift appreciably in the spectra of the complexes. But the position of the thioamide band II of the ligand (1428 cm^{-1}) considerably shifted towards higher wave number side in the complexes ($1460\text{-}1470\text{ cm}^{-1}$). The thioamide band III also shows shift in position in complexes because of coordination of the ligand through sulfur. The thioamide band IV ($760\text{-}790\text{ cm}^{-1}$) in the spectra of the ligand is shifted to lower wave number side in all the complexes [42]. The presence of coordinated water molecules in the metal complexes of (Co(II), Ni(II) and Pt(IV)) is indicated by a broad band in the region

3600-3000 cm^{-1} . These findings clearly indicate that the nature of MMTDT & CBMTDT are bidentate and coordinate through azomethine nitrogen and thiol sulfur atom to the metal [43].

HEMTDT complexes

The band at 1690 cm^{-1} ($\nu_{\text{C=O}}$) of the ligand is observed in the spectra of metal complexes also. This shows the non participation of the carbonyl group in bonding. A strong band at 1620 cm^{-1} in the free ligand was assigned to the azomethine group ($\nu_{\text{N=C-CH}_3}$) which shifts towards $\pm 10-20 \text{ cm}^{-1}$ in the spectra of metal complexes indicating that coordination through nitrogen atom is due to the reduction of double bond character of carbon-nitrogen bond of the azomethine group. Formation of metal-nitrogen bond is further supported by the appearance of a band in the region of 470-480 cm^{-1} in far IR spectra. The existence of thione form of the ligand has been proposed on the basis of a weak band observed for ($\nu_{\text{N-H}}$) around 3200 cm^{-1} and a strong band at 1135-1085 cm^{-1} due to ($\nu_{\text{C=S}}$). However, as expected, in the metal complexes a new band was observed at 750-760 cm^{-1} for ($\nu_{\text{C-S}}$). Metal-sulfur bond formation is further supported by the appearance of a band in the region 320-330 cm^{-1} in the far IR spectra. Four characteristic thioamide bands are expected in the spectra of the ligand and the complexes. The position of the thioamide band I (1530-1560 cm^{-1}) in the spectrum of the ligand is not shift appreciably in the spectra of the complexes. But the position of the thioamide band II of the ligand (1450 cm^{-1}) considerably shifted towards higher wave number side in the complexes (1460-1480 cm^{-1}). The thioamide band III also shows shift in position in complexes because of coordination of the ligand through sulfur. The thioamide band IV (760-790 cm^{-1}) in the spectra of the ligand is shifted to lower wave number side in all the complexes [15]. The presence of coordinated water molecules in the metal complexes of Co(II), Ni(II) and Pt(IV)) is indicated by a broad band in the region 3600-3000 cm^{-1} . These findings clearly indicate that the nature of HEMTDT is bidentate and coordinate through azomethine nitrogen and thiol sulfur atom to the metal.

3.7.2. Electronic absorption spectral Studies

Electronic spectra of the complexes Co(II), Ni(II), Cu(II), Pt(IV) and Pd(II) complexes were taken using DMSO as medium (only representative ones are given as Fig.3.2 B(i-iii)) and the spectral band assignments are given in Table III.3A, 3B & 3C. From Tables and Figures, it is clear that same trend is followed in Co(II), Ni(II), Pt(IV) and Pd(II) complexes of these three ligand systems. For high spin octahedral Co(II) complex, three transitions are expected in the electronic spectra due to ${}^4T_{1g}(F) \rightarrow {}^4T_{2g}(F)$, ${}^4A_{2g}(F)$ and ${}^4T_{1g}(P)$ in the order of increasing energies. The first transition was not recorded but its position was calculated from the second transition. The Racah inter electron repulsion parameter (B), ligand field splitting energy (10Dq) and nephelauxetic parameter (β) for the Co(II) complex have been evaluated [44]. The lower values of B and β of this complex indicate greater orbital overlap and covalency. The Ni(II) complex exhibit three absorption bands for transitions, ${}^3A_{2g}(F) \rightarrow {}^3T_{2g}(F)$, ${}^3T_{1g}(F)$ and ${}^3T_{1g}(P)$, consistent with their well defined octahedral configuration [45]. The ground state of the metal ion Pt(IV) in a strong field octahedral geometry is ${}^1A_{1g}$. The excited state corresponding to t_{2g} and e_g configurations are ${}^3T_{1g}$, ${}^3T_{2g}$, ${}^1T_{1g}$ and ${}^1T_{2g}$ in the increasing order of energy. Thus four transitions can be expected as ${}^1A_{1g} \rightarrow {}^3T_{1g}$, ${}^1A_{1g} \rightarrow {}^3T_{2g}$, ${}^1A_{1g} \rightarrow {}^1T_{1g}$ and ${}^1A_{1g} \rightarrow {}^1T_{2g}$. The positions of the bands observed and probable assignments are given in Table 3 and which agrees octahedral geometry. The Pd(II) complexes show three peaks in the increasing order of frequency corresponding to the transitions ${}^1A_{1g} \rightarrow {}^1A_{2g}$, ${}^1B_{1g}$ and 1E_g . The analytical and spectral data coupled with these results suggest square planar geometry for this complex [46].

The electronic spectra of Cu(II) complex of MMTDT and CBMTDT exhibit same trend in the studies. They exhibit a broad charge transfer band at 36764 cm^{-1} , 25773 cm^{-1} , and two low intensity bands at 14619 cm^{-1} , 14084 cm^{-1} and 14619 cm^{-1} , 13477 cm^{-1} respectively due to ${}^2B_{1g} \rightarrow {}^2E_g$, ${}^2B_{1g} \rightarrow {}^2A_{1g}$ transitions. The electronic spectra of Cu(II) complex of HEMTDT exhibit two charge transfer bands at 31645 cm^{-1} and 25125 cm^{-1} , and shows a low intensity band at 14662 cm^{-1} assigning ${}^2B_{1g} \rightarrow {}^2A_{1g}$

transition, suggesting square-planar geometry for these copper complexes [47-48].

3.7.3 Magnetic Susceptibility Measurements

The magnetic susceptibility studies show that Ni(II), Co(II) and Cu(II) complexes are paramagnetic and all others are diamagnetic. The magnetic moment of octahedral Ni(II) complex is slightly higher than the spin-only value of 2.83 B.M. This difference may be due to either the ferromagnetic interaction in the clusters or Jahn-Teller distortion or spin - orbit coupling or due to the combined effects of all these. The observed magnetic moment of Ni(II) complex is 3.34, 3.02 & 3.12 B.M for MMTDT, CBMTDT & HEMTDT respectively. The results are in good agreement with the reported values of other octahedral nickel(II) complexes [49-50].

The magnetic moments of Co(II) complexes of MMTDT, CBMTDT & HEMTDT are 4.61, 4.70 & 4.72 B.M respectively. These values are slightly higher than expected and is mainly due to the contribution of spin orbit coupling to the magnetic moment [51]. The magnetic moment values obtained for Cu(II) complexes of three ligand systems are 1.68, 1.72 & 1.78 B M respectively, suggesting square planar geometry around Cu(II). [Table III.1A, 1B & 1C].

3.7.4. Electron Spin Resonance Spectra

The ESR spectral studies of Cu(II) complexes provide some information about the metal ion environment. The ESR spectrum of Cu(II) complex of MMTDT, CBMTDT & HEMTDT are recorded at room temperature (27 °C) in solid state, exhibiting an isotropic intense signal giving $g_{iso}=2.10, 2.12$ & 2.07 respectively with no hyperfine splitting (Fig.3.3A, 3B & 3C). This type of spectra was assigned for complexes having large organic substituent as ligand [52-53].

3.7.5. ¹H NMR Spectra

The ¹H NMR spectra of ligand and its zinc complexes have been studied to understand the shift in the δ values due to coordination. The solvent used for

NMR studies was DMSO. The ^1H NMR spectra of Zn(II) complex show a shift of electron density from the ligand to the metal. The involvement of azomethine nitrogen of the ligand molecule in coordination is evident from the change in δ values. In the case of MMTDT, the signal of azomethine protons shielded in the spectra of metal complexes was found to occur at 9 ppm, as compared to its Schiff base at 9.5 ppm. For CBMTDT the signal of azomethine protons de-shielded [54-55] in the spectra of metal complexes was found to occur at 8.3 ppm, as compared to its Schiff base at 9.0 ppm. In HEMTDT the same trend occurs i.e., the signal of azomethine protons de-shielded in the spectra of metal complexes was found to occur at 3.3 and 3.9 ppm, as compared to its Schiff base at 2.4-2.5 ppm. Disappearance of -SH proton in the spectra of the complex supported the deprotonation of the thiol group. The aromatic protons appear as a multiplet at 7.60-8.50 ppm in the ligand and its complexes. The spectra of the ligands and its metal complexes are given in Fig.3.4 B(i-ii).

3.7.6. Thermal Studies

Thermal studies have been performed to examine the presence and nature of water molecules and to study the thermal stability of the metal complexes. In most cases the thermogram exhibited two or more mass loss regions. The thermogram of Co(II) complex of MMTDT show an initial weight loss at 125 $^{\circ}\text{C}$, due to the loss of coordinated water molecule. Corresponding to this weight loss an exotherm is appeared in the DTA at 110 $^{\circ}\text{C}$. The percentage weight loss due to coordinated water molecule obtained from the graph (5.1240) is in good agreement with the theoretical value (5.1350). The mass loss at 200-400 $^{\circ}\text{C}$ is mainly due to the decomposition of organic matter. The major weight loss occurs at 600-1000 $^{\circ}\text{C}$, and mass of the substance unaltered further may be due to the formation of metal oxide. Similar observation is found in Ni(II) and Pt(IV) complexes. In the case of Cu(II) and Zn(II) complexes decomposition take place in two stages. First stage at 200-400 $^{\circ}\text{C}$, due to the decomposition of ligand molecules and second stage at 800-1000 $^{\circ}\text{C}$ due to the formation of metal oxides. The representative DTA

shows endotherms corresponding to these decomposition steps at 220 °C. Similar results are obtained for Cd(II), Hg(II) and Pd(II) complexes also.

The thermogram of Co(II) complex of CBMTDT (Fig.3.5B.i) show an initial weight loss at 100-225 °C, due to the loss of coordinated water molecule. Corresponding to this weight loss an exotherm is appeared in the DTA at 102°C. The percentage weight loss due to coordinated water molecule obtained from the graph (5.4880) is in good agreement with the theoretical value (5.5550). The mass loss at 250-400 °C is mainly due to the decomposition of organic matter. DTA peak corresponding to this mass loss appear at 305 °C. The major weight loss occur at 800-1000 °C, and mass of the substance remain unaltered further, may be due to the formation of metal oxide. Similar observation is found in Ni(II) and Pt(IV) complexes. In the case of Cu(II) and Zn(II) complexes (Fig.3.5B(ii-iii)) decomposition take place in two stages. First stage at 200-400 °C due to decomposition of ligand molecules and second stage at 800-1000 °C due to the formation of metal oxides. The representative DTA shows endotherms corresponding to these decomposition steps at 220 °C. Similar results are obtained for Cd(II), Hg(II) and Pd(II) complexes also.

The thermogram of Co(II) complex of HEMTDT show an initial weight loss at 100-225 °C, due to the loss of coordinated water molecule.. The percentage weight loss due to coordinated water molecule obtained from the graph (5.1000) is in good agreement with the theoretical value (5.2230). The mass loss at 350-400 °C is mainly due to the decomposition of organic matter. The major weight loss occurs at 750-1000 °C, and mass of the substance unaltered further may be due to the formation of metal oxide. Similar observation is found in Ni(II) and Pt(IV) complexes. In the case of Cu(II) and Zn(II) complexes decomposition take place in two stages. First stage at 220-300 °C due to decomposition of ligand molecules and second stage at 800-1000 °C due to the formation of metal oxides. Similar results are obtained for Cd(II), Hg(II) and Pd(II) complexes also.

3.7.7. Fukui Function and Chemical Reactivity

Fukui indices are used for predicting the preferential sites of electrophilic and nucleophilic attack on ligand molecule. Fukui indices widely used as descriptors of site selectivity for the soft-soft reactions. According to Li and Evans, the favorite reactive site is that which possess high value of Fukui indices. For nucleophilic attack the most reactive site of MMTDT, CBMTDT & HEMTDT are on the S(25),N(13), S(25),N(1) & S(23),N(13) atoms respectively and for electrophilic attack the most reactive site is on the N (5),C(14), N (11),C(14) & N (5),C(44) atoms . It is clear that S(25) & S (23) has more nucleophilic character (Table III. 4A, 4B & 4C).

The condensed local softness indices S_k^- and S_k^+ are related to the condensed Fukui functions. The local softness follows the same trend of Fukui functions [56-58]. The results of the theoretical calculations of electron density in the ligand molecule strongly support its site of coordination predicted in the metal complexes using various spectral and physiochemical studies.

3.7.8. Semi empirical Calculations

Semi empirical method is one of the tools for the determination of stability of the molecule by incorporating quantum mechanical parameters into the calculations [59]. The dipole moment, energy of highest occupied molecular orbital (E_{HOMO}), lowest unoccupied molecular orbital (E_{LUMO}), total energy (E_{total}), binding energy (E_{binding}) and heat of formation ($H_{\text{formation}}$) are also calculated and presented in Tables III.5A, 5B & 5C . These calculated geometrical parameters also agree the proposed geometry for the metal complexes [60-61]. The data of selected bond length and bond angles of the Schiff base and its Co(II), Cu(II) and Zn(II) complexes are given in Tables III.6A(i-iii), 6B (i-iii) & 6C(i-iii). The optimized geometry drawn for the lowest energy form of the ligands (Fig.3.6A, 6B & 6C) and metal complexes are given in Fig.3.7A (i-iv), 7B (i-iv) & 7C (i-iv).

3.7.9. Pharmacokinetic Properties (ADME studies)

The pharmacokinetic properties of the ligand and its selected metal complexes are studied using ADME and the results are presented in the Table III 7(A, B & C), 8(A, B & C) & 9 (A, B & C).

3.7.9. 1. Drug likeness

PreADMET is an important tool for predicting drug-likeness and discriminating drug-like compounds and non-drug compounds using certain rules like Lipinski rule/Rule of five, Lead like rule etc. These rules are based on number of hydrogen bond donors, number of hydrogen bond acceptors, molecular weight etc. to test the solubility and permeability of the compounds to act as drug. The obtained results are compared with a standard. From these results (Table III 7A, 7B & 7C) it is clear that the synthesized schiff base ligands obeys most of the rules and exhibit drug like property where as the drug-likeness of the metal complexes are very poor [62-65].

3.7.9. 2. ADME Prediction

Adme means absorption, distribution, metabolism and excretion, which are major part of pharmacokinetics. Among the various in vitro methods of prediction of oral drug absorption, caco-2 cell model and MDCK cell models are quite reliable. Human intestinal absorption data are the sum of bioavailability and absorption, evaluated from the ratio of excretion or cumulative excretion in urine, bile etc. is very important for identifying the drug nature. PreADMET predict the percentage human intestinal absorption (%HIA) of the compounds. The results given in Table III.8A, 8B & 8C shows that only the ligands exhibits fairly good values and all the metal complexes are violating most of the rules and possess out of range values (* marks) and hence decided not to undergo in vivo drug activation studies and discarded [66-69].

3.7.9.3. Toxicity Prediction

Preadmet predicts mutagenicity and carcinogenicity of a compound and helping us to avoid toxic compounds for biological drug likeness studies.

Ames test is a simple method to test mutagenicity of a compound. Generally carcinogenic tests requires long time, PreADMET predicts the results from its model, which is built from the data of NTP (National Toxicology Program) is the results of the in vivo carcinogenicity tests of mice and rat from 2 years. From Tables III 9A, 9B & 9C, it is seen that all the tested compounds show clear evidence of carcinogenic and mutagenic activity and hence rejected [70].

3.8. CONCLUSION

The synthesized Schiff bases MMTDT, CBMTDT & HEMTDT acts as bidentate ligands and coordinate through azomethine nitrogen and thiol sulfur after deprotonation. The bonding and structure of the synthesized complexes were confirmed by analytical, magnetic, spectral and molecular modeling studies. Based on these studies, octahedral geometry is proposed for Co(II), Ni(II), Pt(IV) complexes, square planar for Cu(II), Pd(II) and tetrahedral geometry around Zn(II), Cd(II) and Hg(II) complexes {(Scheme III (i-iv))}. Pharmacokinetic properties of the synthesized Schiff bases and its complexes were studied using Preadmet, and all the metal complexes have been rejected for drug likeness studies.

3.9 REFERENCES

1. Dinku.W, Megersa.N, Raju.V.J.T, Solomon.T, Joensson.J .A & Retta .N, *Bull Chem Soc Ethiop.* 15 (2001) 29.
2. Dinku.W, Megersa.N, Raju.V.J.T, Solomon.T, Joensson.J .A & Retta.N,*Bull Chem Soc Ethiop.* 17 (2003) 33.
3. Mascaros.J.R.G, Clemente -Jun.J.M & Dunbar.K.R, *J. Chem. Soc. Dalton. Trans.* (2002) 2710.
4. Voegtle. F, *Supramolecular chemistry; An introduction, John wiley & sons, New York.* (19991).
5. Lehn .J.M.Lehn, *Supramolecular Chemistry: Concepts and Perspectives, VCH, Germany.* (1995).
6. Milton .M.D & Singh. J.D, *Design and Synthesis of Organoselenium Based Multidonors, IIT, Dept of chemistry, New Delhi.* (2002).
7. Esser .H.O, Dupuis G, Vogel .C, Marco. G. J, Kearney. P.C& Kaufman D.D ,*Herbicides chemistry ,Degradation and mode of action 2nd Edn ,Marcel Dekker Inc New York.* 2 (1976) 129.
8. Dean J.R, Wade G & Barnabas I .J, *J Chrmatography.* 733 (1996) 295.
9. Pacakova.V, Stulik .K & Jiska .J, *J Chrmatography.* 754 (1996) 17.
10. Kebede .B, Retta .N, Raju .V.j.T & Chebude .Y, *Trans. Metal Chem.* 31 (2006) 19
11. Chohan Z.H, Pervez .H, Rauf .A, Khan .K.M, Maharvi .G.M & Supuran.C.T, *J Enzyme Inhib.Med Chem.* 19 (2004) 161.
12. Mashaly .M, Bayoumi .H.A& Taha .A, *Chem Papers Chem Zvesu.* 53 (1999) 299.
13. John .S, Joseph .B, Aravindakshan.K.K & Joseph .A, *Mater chem phys.* 122 (2010) 374.
14. John. S, Joseph .B, Balakrishnan .K.V, Aravindakshan, K.K & Joseph. A, *Mater chem phys.* 123 (2010) 218.

15. Joseph. B, John .S & Joseph .A, *Ind.J.Chem.Tech.* 17 (2010) 425.
16. Saxena .S, Verma. M, Saxena. A.K & Shanker .K, *Arzneim Forsch.* 44 (1994) 766.
17. Davidson .W .M, & Boykin .W.D, *J pharm Sci.* 65 (1978) 737.
18. Mansour.A.K, Awad .S.B&Antown. S. Z, *Natur forsch.* B29 (1974) 792.
19. Heilman. P.W, Gielman .R.D, Scozzie .A.J, Wayner. R.J, Gollo. M.J & Ariyan S.Z , *J. pharm Sci .* 69 (1980) 282.
20. El-Gendy.K & Abdel-Rahman.R.M, *Indian J Heterocycl Chem.* 4 (1995) 293.
21. Labouta .I.M, Eshba .N.H & Salama .H.M, *Farm Sci Ed.* 16 (1988) 29.
22. Abdel-Rahman .R.M, Seada. M, Fawzy .M & El-Baz. I, *Farmaco.* 48 (1993) 397.
23. Korotokikh. N.I, Losev. G.A, Lipnitsky .V.F, Kalisstatov. S.G, Sokolova .A.S & Shavaika .O.P, *Khim-Farm Zh .* 27 (1993) 51.
24. Singh .G, *Synth.React.Inorg Met-Org Chem.* 32 (2002) 171 .
25. Singh. K. *Eur j Med Chem.* 42 (2007) 394.
26. Kandil .S.S, *Trans met Chem.* 27 (2002) 398.
27. Mamatha .K, Mogili .R, Ravinder .M & Srihari .S, *J Ind.Council Chem.* 24 (2007) 4.
28. Burns. G.R, *Inorg.Chem,* 7 (1967) 277.
29. Darnow .A & Menzel .H .P, *Marx Chem Ber.* 97 (1964) 2173.
30. Parr .R.G & Yang .W, *DFT of atoms and molecules, Oxford University Press, Oxford.*(1989).
31. Reed. A. E, Curtiss .L. A & Weinhold. F, *Chem Rev.* 88 (1988) 899.
32. Becke .A.D, *J. Chem. Phys.* 98 (1993) 5648.
33. Lee .W.Y& Parr .R.G, *Phys Rev B.* 37 (1988) 785.
34. F.de. Proft , J.M.L .Martin & P. Geerlings, *Chem Phys Let.t* 256 (1996) 400.

35. Gaur .S & Sharma .B, *J Indian Chem. Soc.* 80 (2003) 841.
36. Gudasi .K.B, Maravalli .P.B &Goudar. T.R, *J Serb Chem Soc* .70 (2005) 643.
37. Sharma .B.D & Bailar .J.C, *J Am Chem Soc.* 77 (1955) 5476.
38. Bellamy. L.J. *The Infrared Spectra of Complex Molecules, third ed., Methuen, London* (1996).
39. Silverstein.R.M, Bassler. G & Morrill. S. *Spectrometric Identification of Organic Compounds, fifth ed. John Wiley and Sons., New York.* (1991).
40. Nakamoto.K, *Infrared Spectra of Inorganic and Coordination Compounds, Part B, fifth ed. Wiley Interscience., New York.* (1997).
41. Kumar.A, Singh.G, Singh.P.A, Singh.K, Handa.R.N ,S.N Dubey & Squattrito P.J, *Proc. Natl. Acad. Sci (India).*72A (II) 87 (2002).
42. Sengupta.S.K, Sahni.S.K & Kapoor.R.N. *React.Inorg.Metal-Org.Chem.* 10 (1980) 269.
43. Kiran .Singh, Barwa. M. S& Tyagi. P, *Euro. J. Med. Chem.* 42 394 (2007).
44. Lever .A.B.P, *Inorganic Electronic spectroscopy, Elsevier., New York* (1968).
45. Khalil .S.M.E, *Chem Paper chem, Zvesti* .54 (2000) 12.
46. Nishat .N, Rahis-ud-din & Dhyani .S, *J. Coord. Chem.* 62 (2009) 996.
47. Vinod.Mathew, Keshavayya.J, Vaidya. V.P& Moinuddinkhan.M.A , *J. of Coord. Chem.* 61 (2008) 2629.
48. Joseph.A & Narayana.B, *J.Indian Chem Soc.* 84 (2007) 746.
49. Cotton.F.A & Wilkinson.G, *Advanced Inorganic chemistry, Interscience. NewYork,* 3 (1972).
50. Lever .A.B.P, *Inorg.Chem.* 4 (1965) 763.
51. Lee J.D, *ELBS. Concise Inorganic Chemistry, 4th Edn, Chapman and Hall Ltd, London.* (1991).

52. Kulkarnia .N.V & Revankara.V. K, *J. Coord. Chem.* 64 (2011) 725.
53. Sathishaa .M.P & Revankara .V.K , *J. Coord. Chem.* 62 (2009) 2540.
54. Singh. K,Barw .M.S & Tyagi .P, *Eur. J. Med. Chem.* 41 (2006) 147.
55. Jhaumeer-Laulloo.B.S & Bhowon. M.G. *Indian J. Chem.* 42A (2003) 2536.
56. Ayers. P.W & Levy .M, *Theor.chem.Acc.* 103 (2000) 353.
57. Geerlings .P& F.De .Proft, *Int J Mol. Sci.* 3 (2002) 276.
58. Li. Y & Evans. J. N .S. *J Am. Chem. Soc.* .117 (1995) 7756.
59. Abdul Jaleel U.C,Rakhila .M & Parameswaran .Geetha, *Advances in Physical Chemistry.* 1 (2010).
60. Serbest.K, Kayi .H, Er. M, Sancak.K & I.De.girmencioglu, *Heteroatom Chemistry.* 19 (2008).
61. Ahamed. A & El-Asmy, *J. Sulphur chemistry.* 3064 (2009).
62. Lipinski .C.A, *Adv. Drug Deliv.Rev.* 23 (1997) 3.
63. Teague .S.J, *Angew Chem.Int.Ed.* 38 (1999) 3743.
64. Oprea .T. I, *J.Comput.Aid.Mol.Des.* 14 (2000) 251.
65. Brown .R.D, *Tools for designing diverse, drug-like cost-effective combinatoriallibraries', in computational library design and Evaluation, Marcel Dekker, Inc., New York.* 328 (2001).
66. Beresford.A.P, *DDT.* 7 (2002) 109.
67. Yamashita. S, *Eur. J Pharm.* 10 (2000) 195.
68. Yazdanian .M, *Pharm Res.* 15 (1998) 1490.
69. Y. Zhao.H, *J.Pharm Sci.* 90 (2001) 749 .
70. Ma .X , *Acta Pharmacologica Sinica.* 26 (2005) 500.

Table III.1A Physical and analytical data of the Schiff base (MMTDT) and its metal complexes

Compounds	μ_{eff} (BM)	Analysis % Found (Calcd.)					M.P ($^{\circ}\text{C}$)
		M	C	H	N	S	
MMTDT $\text{C}_{12}\text{H}_{12}\text{N}_4\text{SO}_2$ (276.00)	-----	-----	59.60 (52.17)	5.98 (4.35)	16.34 (20.28)	9.96 (11.59)	190
$\text{Co}(\text{MMTDT})_2 \cdot 2\text{H}_2\text{O}$ $\text{C}_{24}\text{H}_{26}\text{CoN}_8\text{S}_2\text{O}_6$ (644.93)	4.61	8.95 (9.13)	42.56 (44.66)	3.78 (4.03)	15.89 (17.37)	8.86 (9.92)	>310
$\text{Ni}(\text{MMTDT})_2 \cdot 2\text{H}_2\text{O}$ $\text{C}_{24}\text{H}_{28}\text{NiN}_8\text{S}_2\text{O}_6$ (644.69)	3.34	8.53 (9.10)	43.01 (44.67)	3.56 (4.03)	16.32 (17.37)	8.53 (9.93)	300
$\text{Pt}(\text{MMTDT})_2 \cdot 2\text{H}_2\text{OCl}_2$ $\text{C}_{24}\text{H}_{28}\text{PtN}_8\text{S}_2\text{O}_6\text{Cl}_2$ (852.08)	-----	22.11 (22.89)	32.65 (33.79)	2.36 (3.05)	12.54 (13.14)	7.12 (7.51)	>320
$\text{Cu}(\text{MMTDT})_2$ $\text{C}_{24}\text{H}_{24}\text{CuN}_8\text{S}_2\text{O}_4$ (613.55)	1.68	10.10 (10.35)	45.01 (46.94)	3.24 (3.58)	18.01 (18.25)	9.45 (10.43)	>300
$\text{Pd}(\text{MMTDT})_2$ $\text{C}_{24}\text{H}_{24}\text{PdN}_8\text{S}_2\text{O}_4$ (656.42)	-----	15.20 (16.21)	41.76 (43.87)	2.04 (3.35)	16.57 (17.06)	8.23 (9.75)	>320
$\text{Zn}(\text{MMTDT})_2$ $\text{C}_{24}\text{H}_{24}\text{ZnN}_8\text{S}_2\text{O}_4$ (678.94)	-----	8.59 (9.63)	41.58 (42.42)	3.01 (3.24)	15.14 (16.49)	8.44 (9.43)	>300
$\text{Cd}(\text{MMTDT})_2$ $\text{C}_{24}\text{H}_{24}\text{CdN}_8\text{S}_2\text{O}_4$ (725.96)	-----	14.25 (15.48)	38.25 (39.67)	2.75 (3.03)	14.16 (15.42)	8.01 (8.82)	>280
$\text{Hg}(\text{MMTDT})_2$ $\text{C}_{24}\text{H}_{24}\text{HgN}_8\text{S}_2\text{O}_4$ (750.59)		25.12 (26.72)	36.35 (38.37)	2.11 (2.93)	13.34 (14.92)	8.01 (8.52)	>300

Table III.1B Physical and analytical data of the Schiff base (CBMTDT) and its metal complexes

Compounds	μ_{eff} (B.M)	Analysis % Found (Calcd.)					M.P ($^{\circ}$ C)
		M	C	H	N	S	
CBMTDT $\text{C}_{11}\text{H}_9\text{N}_4\text{SOCl}$ (280.50)		---	46.95 (47.05)	3.28 (3.23)	19.96 (19.96)	10.73 (11.42)	310
Co (CBMTDT) $_2$.2H $_2$ O $\text{C}_{22}\text{H}_{20}\text{CoN}_8\text{S}_2\text{O}_4\text{Cl}_2$ (654.39)	4.70	7.74 (9.01)	38.98 (40.34)	2.98 (3.05)	15.98 (17.12)	8.02 (9.78)	>320
Ni (CBMTDT) $_2$.2H $_2$ O $\text{C}_{22}\text{H}_{20}\text{NiN}_8\text{S}_2\text{O}_4\text{Cl}_2$ (654.15)	3.02	7.43 (8.97)	38.56 (40.35)	2.88 (3.06)	16.02 (17.12)	8.01 (9.78)	>320
Pt (CBMTDT) $_2$.2H $_2$ OCl $_2$ $\text{C}_{22}\text{H}_{20}\text{PtN}_8\text{S}_2\text{O}_4\text{Cl}_4$ (861.54)	----	21.02 (22.64)	28.78 (30.64)	1.55 (2.32)	12.87 (12.99)	7.35 (7.43)	>320
Cu (CBMTDT) $_2$ $\text{C}_{22}\text{H}_{16}\text{CuN}_8\text{S}_2\text{O}_2\text{Cl}_2$ 622.55)	1.72	9.35 (10.20)	40.75 (42.41)	1.96 (2.57)	16.05 (17.99)	9.02 (10.28)	>320
Pd (CBMTDT) $_2$ $\text{C}_{22}\text{H}_{16}\text{PdN}_8\text{S}_2\text{O}_2\text{Cl}_2$ 665.42)	----	13.55 (15.99)	38.04 (39.67)	1.85 (2.40)	15.15 (16.83)	8.29 (9.62)	>320
Zn (CBMTDT) $_2$ $\text{C}_{22}\text{H}_{16}\text{ZnN}_8\text{S}_2\text{O}_2\text{Cl}_2$ 624.39)	----	9.01 (10.47)	40.95 (42.28)	1.98 (2.56)	16.26 (17.94)	9.25 (10.25)	>320
Cd (CBMTDT) $_2$ $\text{C}_{24}\text{H}_{16}\text{CdN}_8\text{S}_2\text{O}_2\text{Cl}_2$ (671.41)	----	15.18 (16.74)	38.03 (39.32)	1.87 (2.38)	15.05 (16.68)	8.01 (9.53)	>320
Hg (CBMTDT) $_2$ $\text{C}_{24}\text{H}_{16}\text{HgN}_8\text{S}_2\text{O}_2\text{Cl}_2$ 759.59)	----	25.15 (26.40)	32.95 (34.76)	1.73 (2.11)	12.94 (14.74)	7.13 (8.42)	>320

Table III.1C Physical and analytical data of the Schiff base (MMTDT) and its metal complexes

Compounds	μ_{eff} (B.M)	Analysis % Found (Calcd.)					M.P ($^{\circ}\text{C}$)
		M	C	H	N	S	
HEMTDT $\text{C}_{12}\text{H}_{12}\text{N}_4\text{SO}_2$ (276.00)	-----	-----	59.60 (52.17)	5.98 (4.35)	16.34 (20.28)	9.96 (11.59)	190
$\text{Co}(\text{HEMTDT})_2 \cdot 2\text{H}_2\text{O}$ $\text{C}_{24}\text{H}_{26}\text{CoN}_8\text{S}_2\text{O}_6$ (644.93)	4.72	8.95 (9.13)	42.74 (44.66)	3.91 (4.03)	15.97 (17.37)	8.85 (9.92)	>310
$\text{Ni}(\text{HEMTDT})_2 \cdot 2\text{H}_2\text{O}$ $\text{C}_{24}\text{H}_{28}\text{NiN}_8\text{S}_2\text{O}_6$ (644.69)	3.12	8.75 (9.10)	43.32 (44.67)	3.87 (4.03)	16.54 (17.37)	8.45 (9.93)	300
$\text{Pt}(\text{HEMTDT})_2 \cdot 2\text{H}_2\text{OCl}_2$ $\text{C}_{24}\text{H}_{28}\text{PtN}_8\text{S}_2\text{O}_6\text{Cl}_2$ (852.08)	-----	22.31 (22.89)	33.54 (33.79)	2.51 (3.05)	12.86 (13.14)	7.01 (7.51)	>320
$\text{Cu}(\text{HEMTDT})_2$ $\text{C}_{24}\text{H}_{24}\text{CuN}_8\text{S}_2\text{O}_4$ (613.55)	1.78	10.87 (10.35)	45.74 (46.94)	3.08 (3.58)	18.01 (18.25)	9.22 (10.43)	>300
$\text{Pd}(\text{HEMTDT})_2$ $\text{C}_{24}\text{H}_{24}\text{PdN}_8\text{S}_2\text{O}_4$ (656.42)	-----	15.20 (16.21)	41.55 (43.87)	2.47 (3.35)	16.23 (17.06)	8.90 (9.75)	>320
$\text{Zn}(\text{HEMTDT})_2$ $\text{C}_{24}\text{H}_{24}\text{ZnN}_8\text{S}_2\text{O}_4$ (678.94)	-----	8.59 (9.63)	41.40 (42.42)	2.88 (3.24)	15.15 (16.49)	8.59 (9.43)	>300
$\text{Cd}(\text{HEMTDT})_2$ $\text{C}_{24}\text{H}_{24}\text{CdN}_8\text{S}_2\text{O}_4$ (725.96)	-----	14.92 (15.48)	38.35 (39.67)	2.61 (3.03)	14.86 (15.42)	7.63 (8.82)	>280
$\text{Hg}(\text{HEMTDT})_2$ $\text{C}_{24}\text{H}_{24}\text{HgN}_8\text{S}_2\text{O}_4$ (750.59)		25.92 (26.72)	37.35 (38.37)	3.61 (2.93)	13.86 (14.92)	7.63 (8.52)	>300

Table III.2 A Infrared spectral data of the MMTDT (L) and its Metal Complexes

Compounds	$\nu(\text{O-H})$ cm^{-1}	$\nu(\text{N-H})$ cm^{-1}	$\nu(\text{C-H})$ cm^{-1}	$\nu(\text{C=O})$ cm^{-1}	$\nu(\text{C=N})$ cm^{-1}	Thioamide I&II cm^{-1}	$\nu(\text{C-O})$ cm^{-1}	Thioamide III cm^{-1}	$\nu(\text{N-N})$ triazine cm^{-1}	Thioamide IV & phenyl with 5 adjacent H cm^{-1}	Aromatic ring cm^{-1}	$\nu(\text{M-N})$ cm^{-1}	$\nu(\text{M-S})$ cm^{-1}
L	----	3320	2900	1680	1601	1540,1420	1350	1190	1050	760	680	---	---
Co(L) ₂ .2H ₂ O	3420	3065	2882	1682	1640	1533,1458	1374	1192	1053	748	675	475	321
Ni(L) ₂ .2H ₂ O	3422	3118	2885	1681	1639	1538,1461	1372	1185	1047	746	682	472	323
Pt(L) ₂ .2H ₂ OCl ₂	3425	3129	2887	1680	1638	1535,1458	1376	1187	1048	750	678	476	320
Cu(L) ₂	----	3062	2890	1682	1639	1532,1473	1378	1195	1046	742	673	477	321
Pd(L) ₂	-----	3110	2892	1681	1642	1536,1452	1373	1186	1053	748	665	482	320
Zn(L) ₂	----	3124	2886	1680	1642	1534,1470	1377	1193	1055	723	670	471	322
Cd(L) ₂	----	3218	2895	1683	1639	1538,1463	1375	1185	1047	721	676	478	320
Hg(L) ₂	----	3114	2884	1680	1630	1532,1462	1372	1195	1046	722	678	477	321

Table III.2B Infrared spectral data of the CBMTDT (L) and its Metal Complexes

Compounds	$\nu(\text{O-H})$ cm^{-1}	$\nu(\text{N-H})$ cm^{-1}	$\nu(\text{C-H})$ cm^{-1}	$\nu(\text{C=O})$ cm^{-1}	$\nu(\text{C=N})$ cm^{-1}	Thioamide I&II cm^{-1}	$\nu(\text{C-O})$ cm^{-1}	Thioamide III cm^{-1}	$\nu(\text{N-N})$ triazine cm^{-1}	Thioamide IV& phenyl with 5 adjacent H cm^{-1}	Aromatic ring cm^{-1}	$\nu(\text{M-N})$ cm^{-1}	$\nu(\text{M-S})$ cm^{-1}
L	----	3310	2913	1698	1611	1540,1428	1350	1164	1051	760	680	---	---
Co(L) ₂ .2H ₂ O	3396	3066	2924	1680	1604	1562,1472	1366	1166	1031	760	682	473	323
Ni(L) ₂ .2H ₂ O	3420	3192	2885	1683	1590	1557,1473	1374	1158	1031	751	685	477	320
Pt(L) ₂ .2H ₂ OCl ₂	3419	3122	2969	1682	1594	1560,1471	1376	1159	1031	754	667	478	323
Cu(L) ₂	----	3065	2922	1681	1590	1541,1471	1376	1173	1032	751	686	478	320
Pd(L) ₂	-----	3022	2922	1680	1593	1538,1472	1376	1159	1030	753	674	485	322
Zn(L) ₂	----	3021	2922	1681	1590	1532,1469	1376	1159	1030	754	673	470	320
Cd(L) ₂	----	3061	2923	1683	1591	1561,1484	1377	1168	1033	754	665	471	323
Hg(L) ₂	----	3064	2871	1684	1590	1560,1470	1377	1157	1032	753	683	471	323

Table III.2C Infrared spectral data of the HEMTDT (L) and its Metal Complexes

Compounds	$\nu(\text{O-H})$ cm^{-1}	$\nu(\text{N-H})$ cm^{-1}	$\nu(\text{C-H})$ cm^{-1}	$\nu(\text{C=O})$ cm^{-1}	$\nu(\text{C=N})$ cm^{-1}	Thioamide I&II cm^{-1}	$\nu(\text{C-O})$ cm^{-1}	Thioamide III cm^{-1}	$\nu(\text{N-N})$ triazine cm^{-1}	Thioamide IV& phenyl with 5 adjacent H cm^{-1}	Aromatic ring cm^{-1}	$\nu(\text{M-N})$ cm^{-1}	$\nu(\text{M-S})$ cm^{-1}
L	----	3263	2900	1690	1620	1541,1451	1300	1160	1024	798	664	---	----
Co(L) ₂ .2H ₂ O	3423	3125	2885	1691	1607	1530,1472	1334	1166	1046	751	676	472	320
Ni(L) ₂ .2H ₂ O	3426	3025	2885	1692	1602	1530,1468	1365	1167	1051	747	682	476	3201
Pt(L) ₂ .2H ₂ OCl ₂	3433	3185	2892	1690	1603	1547,1456	1339	1136	1034	761	656	475	322
Cu(L) ₂	---	3148	2880	1693	1598	1540,1460	1332	1143	1032	754	673	473	323
Pd(L) ₂	----	3023	2885	1690	1598	1536,1467	1333	1140	1032	745	648	478	320
Zn(L) ₂	----	3023	2880	1692	1600	1545,1471	1369	1021	1046	740	678	473	321
Cd(L) ₂	-----	3020	2883	1692	1603	1546,1484	1368	1145	1062	744	654	470	322
Hg(L) ₂	-----	3025	2883	1694	1599	1548,1478	1368	1148	1053	748	652	472	320

Table III.3A Electronic spectral bands and their probable assignment of complexes

Complex	Band Positions (cm ⁻¹)	Assignment	10Dq	B	β
Ni(MMTDT) ₂ .2H ₂ O	12690(Ca)	³ A _{2g} (F) → ³ T _{2g} (F)			
	22842	³ A _{2g} (F) → ³ T _{1g} (F)	12690	821.3	0.78
	27548	³ A _{2g} (F) → ³ T _{1g} (P)			
Co(MMTDT) ₂ .2H ₂ O	8696 (Ca)	⁴ T _{1g} (F) → ⁴ T _{2g} (F)			
	19566	⁴ T _{1g} (F) → ⁴ A _{2g} (F)	10870	934.1	0.96
	20543	⁴ T _{1g} (F) → ⁴ T _{1g} (P)			
Pt(MMTDT) ₂ .2H ₂ OCl ₂	18622(Ca)	¹ A _{1g} → ³ T _{1g}			
	19802	¹ A _{1g} → ³ T _{2g}	20486	214.1	0.36
	23094	¹ A _{1g} → ¹ T _{1g}			
Cu(MMTDT) ₂	14084	² B _{1g} → ² E _g			
	14662	² B _{1g} → ² A _{1g}	-----	-----	-----
	36764	CT			
Pd(MMTDT) ₂	27322(Ca)	¹ A _{1g} → ¹ T _{2g}			
	31847	¹ A _{1g} → ¹ B _{2g}	2732	439.1	0.64
	39370	¹ A _{1g} → ¹ E _{1g}			

Table III.3B Electronic spectral bands and their probable assignment of complexes

Complex	Band Positions (cm ⁻¹)	Assignment	10Dq	B	β
Ni(CBMTDT) ₂ .2H ₂ O	13477(Ca)	³ A _{2g} (F) → ³ T _{2g} (F)			
	17544	³ A _{2g} (F) → ³ T _{1g} (F)	13470	992.7	0.96
	31055	³ A _{2g} (F) → ³ T _{1g} (P)			
Co(CBMTDT) ₂ .2H ₂ O	13513 (Ca)	⁴ T _{1g} (F) → ⁴ T _{2g} (F)			
	14577	⁴ T _{1g} (F) → ⁴ A _{2g} (F)	16890	900.5	0.93
	23641	⁴ T _{1g} (F) → ⁴ T _{1g} (P)			
Pt(CBMTDT) ₂ .2H ₂ OCl ₂	29069 (Ca)	¹ A _{1g} → ³ T _{1g}			
	30120	¹ A _{1g} → ³ T _{2g}	29060	215.1	0.36
	31645	¹ A _{1g} → ¹ T _{1g}			
Cu(CBMTDT) ₂	13477	² B _{1g} → ² E _g			
	14619	² B _{1g} → ² A _{1g}	-----	-----	----
	25773	CT			
Pd(CBMTDT) ₂	14662 (Ca)	¹ A _{1g} → ¹ T _{2g}			
	19150	¹ A _{1g} → ¹ B _{2g}	14660	643.1	0.94
	27239	¹ A _{1g} → ¹ E _{1g}			

Table III. 3C Electronic spectral bands and their probable assignment of complexes

Complex	Band Positions (cm ⁻¹)	Assignment	10Dq	B	β
Ni(HEMTDT) ₂ .2H ₂ O	19157(Ca)	³ A _{2g} (F) → ³ T _{2g} (F)			
	28736	³ A _{2g} (F) → ³ T _{1g} (F)	19157	705.1	0.68
	33557	³ A _{2g} (F) → ³ T _{1g} (P)			
Co(HEMTDT) ₂ .2H ₂ O	18587 (Ca)	⁴ T _{1g} (F) → ⁴ T _{2g} (F)			
	23809	⁴ T _{1g} (F) → ⁴ A _{2g} (F)	23230	953.4	0.98
	28239	⁴ T _{1g} (F) → ⁴ T _{1g} (P)			
Pt(HEMTDT) ₂ .2H ₂ OCl ₂	14705 (Ca)	¹ A _{1g} → ³ T _{1g}			
	20000	¹ A _{1g} → ³ T _{2g}	14700	524.8	0.87
	25512	¹ A _{1g} → ¹ T _{1g}			
Cu(HEMTDT) ₂	14662	² B _{1g} → ² E _g			
	25125	CT	-----	-----	----
	31645	CT			
Pd(HEMTDT) ₂	14534 (Ca)	¹ A _{1g} → ¹ T _{2g}			
	20040	¹ A _{1g} → ¹ B _{2g}	14530	512.5	0.75
	25125	¹ A _{1g} → ¹ E _{1g}			

Table III.4A Fukui functions and local softness values for a nucleophilic and electrophilic for MMTDT

Atom	f ⁻	f ⁺	Sk ⁻	Sk ⁺
1 C	0.0424	0.0369	0.0877	0.0763
2 N	0.0092	0.0520	0.0190	0.1076
3 C	0.0019	0.0990	0.0039	0.2049
4 C	0.0011	0.1456	0.0022	0.3013
5 N	0.0115	0.1868	0.0031	0.2456
6 O	0.0056	0.0689	0.0115	0.1426
7 C	0.0009	0.0015	0.0018	0.0310
8 H	0.0000	0.0044	0.0000	0.0091
9 H	0.0003	0.0046	0.0006	0.0095
10 H	0.0001	0.0000	0.0002	0.0000
11 N	0.0102	0.0206	0.0211	0.0426
12 H	0.0053	0.0001	0.0109	0.0002
13 N	0.0242	0.0661	0.0500	0.1368
14 C	0.0077	0.1192	0.0159	0.2467
15H	0.0012	0.0017	0.0024	0.0035
16C	0.0123	0.0162	0.0254	0.0335
17C	0.0059	0.0357	0.0122	0.0738
18C	0.0041	0.0381	0.0084	0.0788
19C	0.0045	0.0026	0.0093	0.0053
21C	0.0045	0.0014	0.0093	0.0028
22C	0.0109	0.0508	0.0225	0.1051
25S	0.8260	0.0361	1.7098	0.0747
26O	0.0090	0.0094	0.0186	0.0194

Table III.4B Fukui functions and local softness values for a nucleophilic and electrophilic for CBMTDT

Atom	f ⁻	f ⁺	S _k ⁻	S _k ⁺
1 C	0.0450	0.0363	0.0990	0.0799
2 N	0.0112	0.0356	0.0246	0.0783
3 C	0.0024	0.0752	0.0053	0.1654
4 C	0.0008	0.1092	0.0018	0.2402
5 N	0.0122	0.1368	0.0268	0.3009
6 O	0.0071	0.0520	0.0156	0.1144
7 C	0.0008	0.0013	0.0018	0.0029
8 H	0.0001	0.0033	0.0002	0.0073
9 H	0.0002	0.0034	0.0224	0.0075
10 H	0.0001	0.0000	0.0123	0.0000
11 N	0.0102	0.0128	0.9919	0.0282
12 H	0.0056	0.0001	0.0224	0.0002
13 N	0.0203	0.1003	0.0447	0.2207
14 C	0.0065	0.1438	0.0143	0.3164
15 H	0.0016	0.0008	0.0035	0.0018
16 C	0.0024	0.0385	0.0053	0.0847
17 C	0.0013	0.0432	0.0029	0.0950
18 C	0.0022	0.0612	0.0048	0.1346
19 C	0.0006	0.0123	0.0145	0.0271
21 C	0.0001	0.0036	0.0002	0.0079
22 C	0.0026	0.0828	0.0057	0.1822
25 S	0.8646	0.0379	1.9021	0.0834
27 Cl	0.0021	0.0097	0.0046	0.0213

Table III.4C Fukui functions and local softness values for a nucleophilic and electrophilic for HEMTDT

Atom	f ⁻	f ⁺	Sk ⁻	Sk ⁺
1 C	0.0430	0.0342	0.0817	0.0649
2 N	0.0107	0.0529	0.0203	0.1005
3 C	0.0021	0.0977	0.0039	0.1856
4 C	0.0009	0.1448	0.0017	0.2751
5 N	0.0122	0.1866	0.0232	0.3545
6 O	0.0053	0.0743	0.0101	0.1412
7 C	0.0009	0.0015	0.0017	0.0029
8 H	0.0001	0.0046	0.0002	0.0087
9 H	0.0002	0.0045	0.0004	0.0086
10 H	0.0001	0.0000	0.0002	0.0000
11 N	0.0103	0.0214	0.0196	0.0407
12 H	0.0057	0.0001	0.0108	0.0002
13 N	0.0267	0.0529	0.0507	0.1005
14 C	0.0074	0.0940	0.0141	0.1786
15C	0.0033	0.0272	0.0063	0.0517
16C	0.0030	0.0282	0.0057	0.0536
17C	0.0015	0.0436	0.0029	0.0828
18C	0.0001	0.0114	0.0002	0.0217
19C	0.0011	0.0032	0.0021	0.0061
20C	0.0038	0.0667	0.0072	0.1267
23S	0.8564	0.0328	1.6272	0.0623
26O	0.0015	0.0043	0.0029	0.0082
28C	0.0027	0.0048	0.0051	0.0091

Table III.5A Calculation of energy parameters of Schiff base (MMTDT) and its metal complexes by using semi empirical methods (PM3) units Kcal/mol.

Compds	E _{Total} Kcal/mol	E _{Binding} Kcal/mol	H _{Formation} Kcal/mol	E _{Homo} Kcal/mol	E _{Lumo} Kcal/mol	Dipolemoment (D)
MMTDT	-69768.6875	-3255.4577	-57.9643	-9.2525	-1.4700	3.1040
Ni	-178625.2344	-7250.2544	-193.0854	-8.1372	-0.9712	4.8870
Co	-172916.6406	-7407.1123	-350.3421	-8.1372	-0.9712	3.3760
Zn	-140242.1719	-6584.1372	-73.8767	-7.8143	-1.4260	9.4158
Cd	-140096.1406	-6551.9609	-101.6031	-7.9889	-1.1850	5.0860
Cu	-166948.7344	-6714.3066	-6.7628	-7.2308	-1.5570	6.5330
Hg	-140256.9375	-6564.0209	-77.5129	-7.7378	-1.3130	9.3120
Pd	-163868.9375	-6940.0620	-223.2180	-8.3367	-1.2370	7.0250

Table III.5B Calculation of energy parameters of Schiff base (CBMTDT) and its metal complexes by using semiempirical methods (PM3) units Kcal/mol.

Compds	E _{Total} Kcal/mol	E _{Binding} Kcal/mol	H _{Formation} Kcal/mol	E _{Homo} Kcal/mol	E _{Lumo} Kcal/mol	Dipolemoment(D)
CBMTDT	-66504.2891	-2864.3718	-91.2851	-9.3041	-1.5240	3.0810
Ni	-172097.8906	-6469.5288	-127.8889	-7.6965	-1.2330	3.7170
Co	-166389.7031	-6626.778	-285.5385	-8.0530	-1.6430	4.6300
Zn	-133712.0156	-5800.6074	-73.8767	-7.8601	-1.6450	8.9540
Cd	-133567.5469	-5769.9809	-168.0531	-8.0535	-1.2470	4.0350
Cu	-160420.7344	-5932.9263	-59.0876	-7.2547	-1.6100	6.6130
Hg	-133726.5938	-5780.2852	-145.7188	-7.7670	-1.6340	8.7880
Pd	-157258.1250	-6075.8574	-74.5436	-7.5741	-1.8870	5.3650

Table III.5C Calculation of energy parameters of Schiff base (HEMTDT) and its metal complexes by using semi empirical methods (PM3) units Kcal/mol.

Compds	E _{Total} Kcal/mol	E _{Binding} Kcal/mol	H _{Formation} Kcal/mol	E _{Homo} Kcal/mol	E _{Lumo} Kcal/mol	Dipolemoment(D)
HEMTDT	-69780.86719	-3267.6398	-45.7822	-9.2618	-1.5050	2.7360
Ni	-178635.125	-7260.1376	-202.9678	-7.9498	-0.9295	4.4700
Co	-172943.375	-7433.8398	-377.0696	-7.7099	-1.3410	2.1570
Zn	-140254.9688	-6596.9379	-61.0761	-7.9687	-1.1720	8.6380
Cd	-140120.6094	-6576.4316	-77.1324	-8.2037	-1.2920	2.3810
Cu	-166970.875	-6736.4585	-28.9841	-7.5274	-1.2370	6.9950
Hg	-140280.5313	-6587.6162	-53.9375	-7.8856	-1.2130	8.7700
Pd	-163849.0156	-6920.1318	-203.2877	-8.2429	-1.3480	3.6790

Table III.6A.i The selected bond lengths and the bond angles calculated for MMTDT.

Bond length	(Å)	Bond angle	(°)
C(7)-N(6)	1.2901	N(1)-C(17)-S(15)	126.337
N(1)-N(6)	1.4476	N(6)-N(1)-C(17)	117.080
C(17)-S(15)	1.6414	N(6)-N(1)-C(7)	123.349
C(17)-N(1)	1.4207		

Table III.6A.ii The selected bond lengths and the bond angles calculated for the cobalt(II) complex.

Bond length	(Å)	Bond angle	(°)
Co(34)-O(65)	1.9856	N(23)- Co(34)-S(15)	92.9716
Co(34)-O(64)	2.0057	S(32)- Co(34)-O(65)	87.1394
Co(34)-S(15)	2.2641	O(64)- Co(34)-O(65)	77.5328
Co(34)-S(32)	2.2696	O(64)- Co(34)-S(32)	84.7225
Co(34)-N(6)	1.8597	S(32)- Co(34)-N(6)	93.8813
Co(34)-N(23)	1.8797	N(23)- Co(34)-N(6)	97.8466
C(7)-N(6)	1.4132	S(32)- Co(34)-S(15)	173.3030
C(24)-N(23)	1.3111	N(23)- C(34)-O(65)	174.1800
N(1)-N(6)	1.4843	N(6)- Co(34)-O(65)	87.5114
N(23)-N(19)	1.4773	N(23)- Co(34)-O(64)	97.1487
C(35)-S(15)	1.7507	N(6)- Co(34)-O(64)	164.9900
C(21)-S(32)	1.7307	N(23)- Co(34)-S(32)	90.2193
C(21)-N(19)	1.4519	Co(34)-N(23)-N(19)	113.9180
C(35)-N(1)	1.4369	Co(34)-N(6)-N(1)	115.7470
		Co(34)-S(15)-C(35)	95.3083
		Co(34)-S(32)-C(21)	94.4137
		N(1)-C(35)-S(15)	118.1260
		N(19)-C(21)-S(32)	120.1900
		N(23)-N(19)-C(21)	113.0710
		N(6)-N(1)-C(35)	116.0780
		N(6)-Co(34)-S(15)	91.5156
		S(15)-Co(34)-O(65)	89.1385
		S(15)-Co(34)-O(64)	87.0390

Table III.6A.iii The selected bond lengths and the bond angles calculated for the copper(II) complex.

Bond length	(Å)	Bond angle	(°)
Cu(34)-S(32)	2.0759	N(23)- Cu(34)-S(15)	112.2660
Cu(34)-S(15)	2.1717	S(32)- Cu(34)-N(6)	131.3150
Cu(34)-N(6)	1.9099	N(23)- Cu(34)-N(6)	113.0300
Cu(34)-N(23)	1.9829	S(32)- Cu(34)-S(15)	119.5060
C(7)-N(6)	1.3002	N(23)- Cu(34)-S(32)	93.9373
C(24)-N(23)	1.3138	N(6)- Cu(34)-S(32)	112.8760
N(1)-N(6)	1.4941	Cu(34)-N(23)-N(19)	123.8160
N(23)-N(19)	1.5214	Cu(34)-N(6)-N(1)	99.3155
C(35)-S(15)	1.7722	Cu(34)-S(15)-C(35)	97.5532
C(21)-S(32)	1.7483	Cu(34)-S(32)-C(21)	120.9530
C(21)-N(19)	1.4516	N(1)-C(35)-S(15)	122.8550
C(35)-N(1)	1.4579	N(19)-C(21)-S(32)	111.6320
		N(23)-N(19)-C(21)	108.1050
		N(6)-N(1)-C(35)	

Table III.6A.iv The selected bond lengths and the bond angles calculated for the zinc(II) complex.

Bond length	(Å)	Bond angle	(°)
Zn(34)-S(32)	2.3109	N(23)- Zn(34)-S(15)	116.3640
Zn(34)-S(15)	2.3115	S(32)- Zn(34)-N(6)	116.2970
Zn(34)-N(6)	2.1147	N(23)- Zn(34)-N(6)	115.8370
Zn(34)-N(23)	2.1119	S(32)- Zn(34)-S(15)	131.4600
C(7)-N(6)	1.3069	N(23)- Zn(34)-S(32)	89.5510
C(24)-N(23)	1.3078	Zn(34)-N(23)-N(19)	114.4670
N(1)-N(6)	1.4413	Zn(34)-N(6)-N(1)	114.3880
N(23)-N(19)	1.4418	Zn(34)-S(15)-C(35)	93.0755
C(35)-S(15)	1.7431	Zn(34)-S(32)-C(21)	93.1246
C(21)-S(32)	1.7431	N(1)-C(35)-S(15)	128.4150
C(21)-N(19)	1.4562	N(19)-C(21)-S(32)	128.4420
C(35)-N(1)	1.4563	N(23)-N(19)-C(21)	113.3490
		N(6)-N(1)-C(35)	113.5060

Table III.6B.i The bond lengths and the bond angles calculated for the ligand CBMTDT

Bond length	(Å)	Bond angle	(°)
C(7)-N(6)	1.2896	N(1)-C(18)-S(16)	126.1531
N(1)-N(6)	1.4476	N(6)-N(1)-C(18)	116.7590
C(18)-S(16)	1.6414	N(1)-N(6)-C(7)	123.8724
C(18)-N(1)	1.4269		

Table III.6B.ii The selected bond lengths and the bond angles calculated for the cobalt(II) complex.

Bond length	(Å ^o)	Bond angle	(^o)
Co(36)-O(38)	2.0047	N(6)- Co(36)-S(16)	91.5109
Co(36)-O(37)	1.9838	N(6)- Co(36)-S(33)	93.9506
Co(36)-S(16)	2.2649	N(24)- Co(36)-S(33)	90.2547
Co(36)-S(33)	2.2699	N(24)- Co(36)-S(16)	92.371
Co(36)-N(6)	1.8600	S(16)- Co(36)-O(37)	89.8927
Co(36)-N(24)	1.8795	S(16)- Co(36)-O(38)	87.1078
C(7)-N(6)	1.4087	S(33)- Co(36)-O(38)	86.7396
C(25)-N(24)	1.3111	S(33)- Co(36)-O(37)	86.9048
N(1)-N(6)	1.4814	N(6)- Co(36)-O(37)	88.3005
N(20)-N(24)	1.4757	N(6)- Co(36)-O(38)	164.8310
C(39)-S(16)	1.7496	N(24)- Co(36)-O(37)	173.6780
C(22)-S(33)	1.7268	N(24)- Co(36)-O(38)	97.6146
C(22)-N(20)	1.4519	N(24)- Co(36)-N(6)	97.5351
C(39)-N(1)	1.4399	S(16)- Co(36)-S(33)	173.5820
		O(16)- Co(36)-O(33)	76.5973
		Co(36)-N(24)-N(20)	113.0590
		Co(36)-N(6)-N(1)	115.0080
		Co(36)-S(33)-C(22)	93.8263
		Co(36)-S(16)-C(39)	95.2758
		N(20)-C(22)-S(33)	120.6150
		N(1)-C(39)-S(16)	117.7880
		N(24)-N(20)-C(22)	113.0780
		N(6)-N(1)-C(39)	116.0300

Table III.6B.iii The selected bond lengths and the bond angles calculated for the copper(II) complex.

Bond length	(Å ^o)	Bond angle	(^o)
Cu(34)-S(32)	1.7241	N(23)- Cu(34)-S(15)	128.7310
Cu(34)-S(15)	2.0736	S(32)- Cu(34)-N(6)	112.5530
Cu(34)-N(6)	1.9688	N(23)- Cu(34)-N(6)	114.4860
Cu(34)-N(23)	1.9065	S(32)- Cu(34)-S(15)	119.0490
C(7)-N(6)	1.3155	N(23)- Cu(34)-S(32)	88.3858
C(24)-N(23)	1.3019	N(6)- Cu(34)-S(32)	112.5530
N(1)-N(6)	1.5164	Cu(34)-N(23)-N(19)	122.7810
N(23)-N(19)	1.4966	Cu(34)-N(6)-N(1)	112.3110
C(35)-S(15)	1.7425	Cu(34)-S(15)-C(35)	96.8632
C(21)-S(32)	1.7664	Cu(34)-S(32)-C(21)	98.8847
C(21)-N(19)	1.4586	N(1)-C(35)-S(15)	122.9880
C(35)-N(1)	1.4533	N(19)-C(21)-S(32)	121.1300
		N(23)-N(19)-C(21)	108.5360
		N(6)-N(1)-C(35)	112.0990

Table III.6B.iv The selected bond lengths and the bond angles calculated for the zinc(II) complex.

Bond length	(Å)	Bond angle	(°)
Zn(34)-S(32)	2.3095	N(23)- Zn(34)-S(15)	117.7770
Zn(34)-S(15)	2.3095	S(32)- Zn(34)-N(6)	118.0690
Zn(34)-N(6)	2.1144	N(23)- Zn(34)-N(6)	114.2250
Zn(34)-N(23)	2.1151	S(32)- Zn(34)-S(15)	129.7640
C(7)-N(6)	1.3081	N(23)- Zn(34)-S(32)	89.5618
C(24)-N(23)	1.3080	N(6)- Zn(34)-S(32)	118.0690
N(1)-N(6)	1.4388	Zn(34)-N(23)-N(19)	114.2590
N(23)-N(19)	1.4388	Zn(34)-N(6)-N(1)	114.3030
C(35)-S(15)	1.7434	Zn(34)-S(15)-C(35)	93.1382
C(21)-S(32)	1.7436	Zn(34)-S(32)-C(21)	93.1292
C(21)-N(19)	1.4566	N(1)-C(35)-S(15)	128.3200
C(35)-N(1)	1.4567	N(19)-C(21)-S(32)	128.3090
		N(23)-N(19)-C(21)	113.7590
		N(6)-N(1)-C(35)	113.7720

Table III.6C.i The selected bond lengths and the bond angles calculated for the ligand HEMTDT.

Bond length	(Å)	Bond angle	(°)
C(7)-N(6)	1.3006	N(1)-C(18)-S(16)	126.5580
N(1)-N(6)	1.4412	N(6)-N(1)-C(18)	116.7682
C(18)-S(16)	1.6366	N(6)-N(1)-C(7)	105.7744
C(18)-N(1)	1.4237		

Table III.6C.ii The selected bond lengths and the bond angles calculated for the nickel(II) complex.

Bond length	(Å ^o)	Bond angle	(^o)
Ni (35)-O(36)	1.9233	N(24)-Ni(35)-S(16)	89.2005
Ni (35)-O(37)	1.9292	N(24)-Ni(35)-S(33)	94.0007
Ni (35)-S(33)	2.2881	N(6)-Ni(35)-S(33)	83.2893
Ni (35)-S(16)	2.2796	N(6)-Ni(35)-S(16)	93.5401
Ni (35)-N(6)	1.8523	S(33)-Ni(35)-O(36)	86.2905
Ni (35)-N(24)	1.8484	S(33)-Ni(35)-O(37)	93.4832
C(6)-N(7)	1.4324	S(16)-Ni(35)-O(36)	91.8444
C (25)-N(24)	1.4477	S(16)-Ni(35)-O(37)	88.7631
N(1)-N(6)	1.4899	N(6)-Ni(35)-O(36)	94.9474
N(20)-N(24)	1.4747	N(6)-Ni(35)-O(37)	159.9784
C(38)-S(16)	1.7077	N(24)-Ni(35)-O(36)	152.5810
C(22)-S(33)	1.7155	N(24)-Ni(35)-O(37)	87.5585
C(38)-N(1)	1.4405	N(6)-Ni(35)-N(24)	112.3391
C(22)-N(20)	1.4391	S(16)-Ni(35)-S(33)	176.1620
		O(36)-Ni(35)-O(37)	65.0824
		Ni(35)-N(6)-N(1)	65.0824
		Ni(35)-N(20)-N(24)	110.4034
		Ni(35)-S(16)-C(38)	87.6356
		Ni(35)-S(33)-C(22)	93.1140
		N(1)-C(38)-S(16)	120.2591
		N(20)-C(22)-S(33)	117.9162
		N(6)-N(1)-C(38)	118.6450
		N(24)-N(20)-C(22)	119.2394

Table III.6C.iii The selected bond lengths and the bond angles calculated for the copper(II) complex.

Bond length	(Å ^o)	Bond angle	(^o)
Cu(35)-S(33)	2.2032	N(24)- Cu (35)-S(16)	140.0630
Cu (35)-S(16)	2.1708	S(33)- Cu (35)-N(6)	96.6882
Cu (35)-N(6)	2.0313	N(24)- Cu (35)-N(6)	129.2730
Cu (35)-N(24)	1.9325	S(33)- Cu (35)-S(16)	95.5247
C(7)-N(6)	1.3281	N(24)- Cu (35)-S(33)	83.3797
C (25)-N(24)	1.3134	N(6)- Cu (35)-S(16)	90.5964
N(1)-N(6)	1.5342	Cu (35)-N(24)-N(20)	128.2500
N(24)-N(20)	1.4919	Cu (35)-N(6)-N(1)	114.2440
C(36)-S(16)	1.7535	Cu (35)-S(16)-C(36)	99.0076
C(22)-S(33)	1.7756	Cu (35)-S(33)-C(22)	102.2130
C(22)-N(20)	1.4580	N(1)-C(36)-S(16)	122.1020
C(36)-N(1)	1.4486	N(20)-C(22)-S(33)	119.3210
		N(24)-N(20)-C(22)	106.4710
		N(6)-N(1)-C(36)	113.1830

Table III.6C.iv The selected bond lengths and the bond angles calculated for the zinc(II) complex.

Bond length	(Å)	Bond angle	(°)
Zn(35)-S(33)	2.3227	N(24)- Zn (35)-S(16)	116.2192
Zn (35)-S(16)	2.3219	S(33)- Zn (35)-N(6)	116.1244
Zn (35)-N(6)	2.1585	N(24)- Zn (35)-N(6)	119.0831
Zn (35)-N(24)	2.1524	S(33)- Zn (35)-S(16)	129.0680
C(7)-N(6)	1.3142	N(24)- Zn (35)-S(33)	89.7385
C (25)-N(24)	1.3140	N(6)- Zn (35)-S(16)	89.6727
N(1)-N(6)	1.4403	Zn (35)-N(24)-N(20)	112.9633
N(24)-N(20)	1.4443	Zn (35)-N(6)-N(1)	129.5781
C(36)-S(16)	1.7405	Zn (35)-S(16)-C(36)	92.2550
C(22)-S(33)	1.7411	Zn (35)-S(33)-C(22)	92.3499
C(22)-N(20)	1.4586	N(1)-C(36)-S(16)	128.2721
C(36)-N(1)	1.4598	N(20)-C(22)-S(33)	128.2920
		N(24)-N(20)-C(22)	113.7111
		N(6)-N(1)-C(36)	113.6560

Table III.7A Results of Drug likeness studies of Schiff base, MMTDT (L) and its metal complexes

Basic information	L	Co	Ni	Zn	Cu	Pt	STD
CMC like Rule	Qualified	Failed	Failed	Failed	Failed	Failed	Qualified
CMC like Rule violations	0	4	4	2	2	4	0
Lead like Rule	Suitable if its binding affinity >0.1µM	Violated	Violated	Violated	Violated	Violated	Violated
Lead like Rule Violations	0	2	2	2	2	2	2
MDDR like Rule	Mid-structure	Mid-structure	Mid-structure	Mid-structure	Mid-structure	Mid-structure	Mid-structure
MDDR like Rule Violations	2	1	1	1	1	1	1
Rule of five	Suitable	Suitable	Suitable	Suitable	Suitable	Suitable	Suitable
Rule of Five Violations	0	1	1	1	1	1	0
WDI like Rule	In 90% cutoff	Failed	Failed	Failed	Failed	Failed	
WDI like Rule Violations	0	10	10	10	10	10	10

STD-Ampicillin

Table III.7B Results of Drug likeness studies of Schiff base, CBMTDT (L) and its metal complexes

Basic information	L	Co	Ni	Zn	Cu	Pt	STD
CMC like Rule	Qualified	Failed	Failed	Failed	Failed	Failed	Qualified
CMC like Rule violations	0	3	3	2	2	3	0
Lead like Rule	Suitable if its binding affinity >0.1 μ M	Violated	Violated	Violated	Violated	Violated	Violated
Lead like Rule Violations	0	2	2	2	2	2	2
MDDR like Rule	Mid-structure	Mid-structure	Mid-structure	Mid-structure	Mid-structure	Mid-structure	Mid-structure
MDDR like Rule Violations	2	1	1	1	1	1	1
Rule of five	Suitable	Suitable	Suitable	Suitable	Suitable	Suitable	Suitable
Rule of Five Violations	0	1	1	1	1	1	0
WDI like Rule	In 90% cutoff	Failed	Failed	Failed	Failed	Failed	In 90% cutoff
WDI like Rule Violations	0	10	10	10	10	10	0

STD-Ampicillin

Table III.7C Results of Drug likeness studies of Schiff base, HEMTDT (L) and its metal complexes

Basic information	L	Co	Ni	Zn	Cu	Pt	STD
CMC like Rule	Qualified	Failed	Failed	Failed	Failed	Failed	Qualified
CMC like Rule violations	0	4	4	4	3	4	0
Lead like Rule	Suitable if its binding affinity >0.1 μ M	Violated	Violated	Violated	Violated	Violated	Violated
Lead like Rule Violations	0	2	2	2	2	2	2
MDDR like Rule	Mid-structure	Mid-structure	Mid-structure	Mid-structure	Mid-structure	Mid-structure	Mid-structure
MDDR like Rule Violations	2	1	1	1	1	1	1
Rule of five	Suitable	Suitable	Suitable	Suitable	Suitable	Suitable	Suitable
Rule of Five Violations	0	1	1	1	1	1	0
WDI like Rule	In 90% cutoff	Failed	Failed	Failed	Failed	Failed	In 90% cutoff
WDI like Rule Violations	0	10	10	10	10	10	1

STD-Ampicillin

Table III.8A. Results of Adme calculation of Schiff base, MMTDT (L) and its metal complexes

Result of calculation	L	Co	Ni	Zn	Cu	Pt	STD
Absorption							
Human intestinal absorption (HIA, %)	96.9001	99.5452**	99.6520**	99.0071**	99.0025**	99.8816**	81.4784
in vitro Caco-2 cell permeability(nm/sec)	20.5015	3.7772**	3.3499**	20.6752**	20.6998**	4.5885**	0.6307
in vitro MDCK cell permeability(nm/sec)	59.1189	0.4581*	0.4577*	0.2109*	0.2017*	0.5185*	0.9376
in vitro skin permeability(logKp,cm/hour)	-3.8185	-4.9753**	-5.0069**	-52268**	-5.2381**	-2.5524**	-5.0357
Distribution(2 Items)							
in vitro plasma protein binding (%)	71.5100	72.3551**	72.431**	18.3804**	18.3710**	72.3964**	36.547
in vivo blood-brain barrier penetration (C.brain/C.blood)	0.1650	0.0384**	0.0384**	0.0488**	0.0488**	0.0384**	0.0588

*out of range, STD-Ampicillin

Table III.8B Results of Adme calculation of Schiff base, CBMTDT (L) and its metal complexes

Result of calculation	L	Co	Ni	Zn	Cu	Pt	STD
Absorption							
Human intestinal absorption (HIA, %)	97.8976	100.0000**	100.0000**	97.8029**	97.8035**	99.8571**	81.4784
in vitro Caco-2 cell permeability(nm/sec)	18.6425	1.6711**	1.5088**	22.1104**	22.2792**	4.6943**	0.6307
in vitro MDCK cell permeability(nm/sec)	173.2030	0.4887*	0.4884*	0.3351*	0.3264*	0.5185*	0.9376
in vitro skin permeability(logKp,cm/hour)	-3.62544	-4.7091**	-4.9811**	-5.2265**	-5.2377**	-2.5700**	-5.0357
Distribution(2 Items)							
in vitro plasma protein binding (%)	84.3425	70.2679**	69.3443**	21.3688**	21.3996**	69.2163**	36.1547
in vivo blood-brain barrier penetration (C.brain/C.blood)	1.0414	0.0417**	0.0417**	0.0674**	0.0674**	0.0417**	0.0588

*out of range, STD-Ampicillin

Table III. 8C Results of Adme calculation of Schiff base, HEMTDT (L)) and its metal complexes

Result of calculation	L	Co	Ni	Zn	Cu	Pt	STD
Absorption							
Human intestinal absorption (HIA, %)	93.9289	99.5386**	99.6460**	99.0562**	99.05159**	99.8774**	81.4784
in vitro Caco-2 cell permeability(nm/sec)	20.3509	0.8758**	0.8275**	19.3901**	19.2985**	0.9503**	0.6307
in vitro MDCK cell permeability(nm/sec)	19.6555	0.5161*	0.5161*	0.5050*	0.5047*	0.5185*	0.9376
in vitro skin permeability(logKp,cm/hour)	-3.8632	-4.2022**	-4.6678**	-5.2422**	-5.2661**	-4.1285**	-5.0357
Distribution(2 Items)							
in vitro plasma protein binding (%)	61.6769	71.1945**	71.1388**	24.3341**	24.3237**	71.2095**	36.1547
in vivo blood-brain barrier penetration (C.brain/C.blood)	0.4217	0.0390**	0.0390**	0.0520**	0.0520**	0.0390**	0.0588

*out of range, STD-Ampicillin

Table III.9A Results of Toxicity calculation of schiff base MMTDT (L) and its complexes

Result of calculation	L	Co	Ni	Zn	Cu	Pt	STD
Ames test							
Ames TA100 (+S9)	+ve	-ve	-ve	-ve	-ve	-ve	-ve
Ames TA100 (-S9)	+ve	-ve	-ve	-ve	-ve	-ve	-ve
Ames TA1535 (+S9)	+ve	-ve	-ve	-ve	-ve	-ve	+ve
Ames TA1535 (-S9)	-ve	+ve	+ve	+ve	+ve	+ve	-ve
Ames TA98 (+S9)	+ve	out of range	out of range	out of range	out of range	out of range	-ve
Ames TA98 (-S9)	+ve	-ve	-ve	-ve	-ve	-ve	-ve
Ames test	mutagen	mutagen	mutagen	mutagen	mutagen	mutagen	mutagen
Carcinogenicity							
Carcinogenicity(Mouse)	-ve	out of range	out of range	out of range	out of range	out of range	+ve
Carcinogenicity (Rat)	-ve	out of range	out of range	out of range	out of range	out of range	+ve

Table III.9B Results of Toxicity calculation of schiff base CBMTDT (L) and its complexes

Result of calculation	L	Co	Ni	Zn	Cu	Pt	STD
Ames test							
Ames TA100 (+S9)	+ve	-ve	-ve	+ve	+ve	-ve	-ve
Ames TA100 (-S9)	+ve	-ve	-ve	-ve	-ve	-ve	-ve
Ames TA1535 (+S9)	+ve	-ve	-ve	-ve	-ve	-ve	+ve
Ames TA1535 (-S9)	-ve	+ve	+ve	+ve	+ve	+ve	-ve
Ames TA98 (+S9)	+ve	out of range	out of range	out of range	out of range	out of range	-ve
Ames TA98 (-S9)	+ve	-ve	-ve	-ve	-ve	-ve	-ve
Ames test	mutagen	mutagen	mutagen	mutagen	mutagen	mutagen	mutagen
Carcinogenicity							
Carcinogenicity(Mouse)	+ve	out of range	out of range	out of range	out of range	out of range	+ve
Carcinogenicity (Rat)	-ve	out of range	out of range	out of range	out of range	out of range	+ve

STD –Nystatin

Table III. 9C Results of Toxicity calculation of Schiff base HEMTDT (L) and its complexes

Result of calculation	L	Co	Ni	Zn	Cu	Pt	STD
Ames test							
Ames TA100 (+S9)	+ve	-ve	-ve	-ve	-ve	-ve	-ve
Ames TA100 (-S9)	-ve	-ve	-ve	-ve	-ve	-ve	-ve
Ames TA1535 (+S9)	+ve	-ve	-ve	-ve	-ve	-ve	+ve
Ames TA1535 (-S9)	-ve	-ve	-ve	-ve	-ve	-ve	-ve
Ames TA98 (+S9)	+ve	out of range	out of range	out of range	out of range	out of range	-ve
Ames TA98 (-S9)	+ve	-ve	-ve	-ve	-ve	-ve	-ve
Ames test	mutagen	mutagen	non-mutagen	non-mutagen	non-mutagen	non-mutagen	mutagen
Carcinogenicity(2 Items)							
Carcinogenicity(Mouse)	-ve	out of range	out of range	out of range	out of range	out of range	+ve
Carcinogenicity (Rat)	-ve	out of range	out of range	out of range	out of range	out of range	+ve

STD -Nystatin

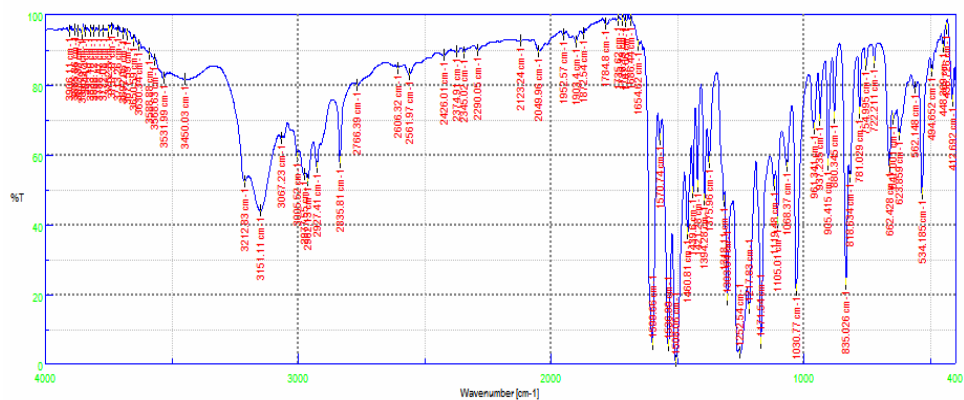


Fig. 3.1A.i The infrared spectrum of the Schiff base (MMTDT)

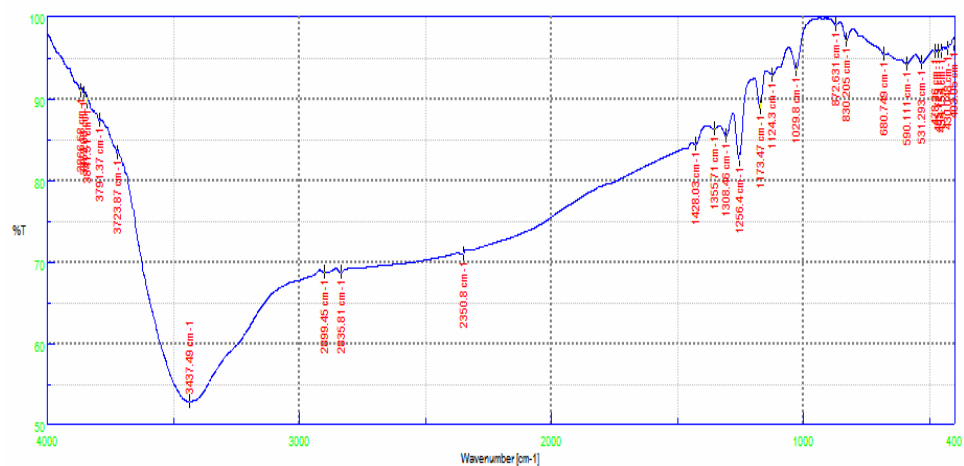


Fig.3.1A.ii The infrared spectrum of the cobalt complex

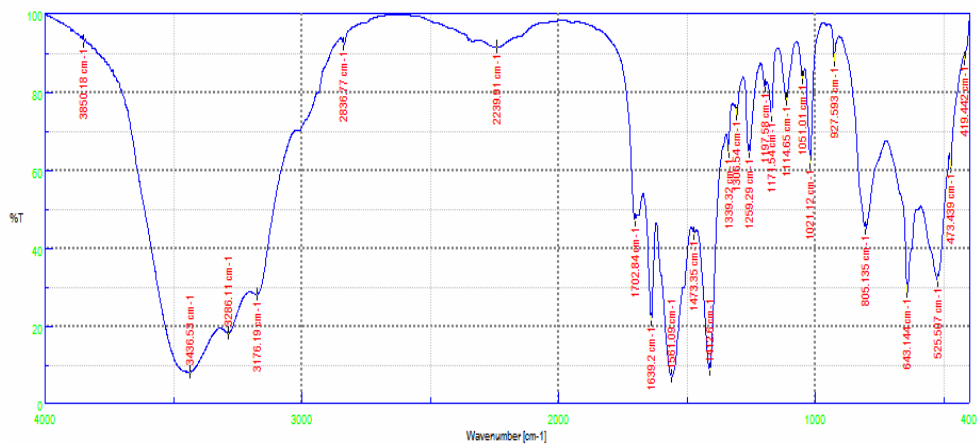


Fig.3.1A .iii The infrared spectrum of the copper complex

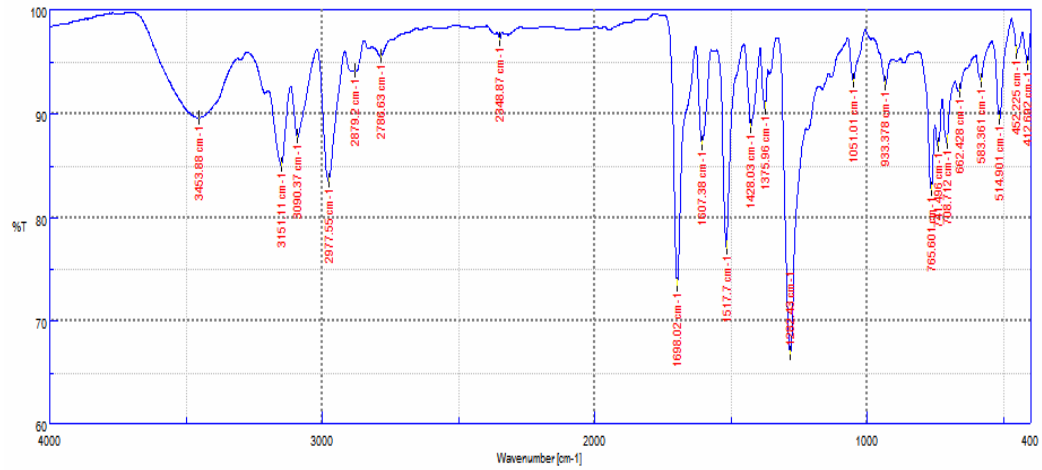


Fig.3.1B.i The infrared spectrum of the Schiff base (CBMTDT)

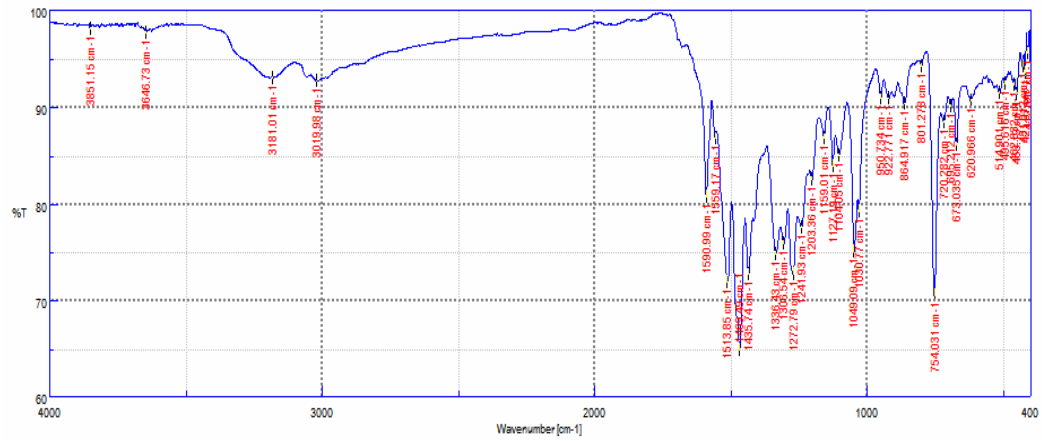


Fig.3.1B.ii The infrared spectrum of the zinc complex

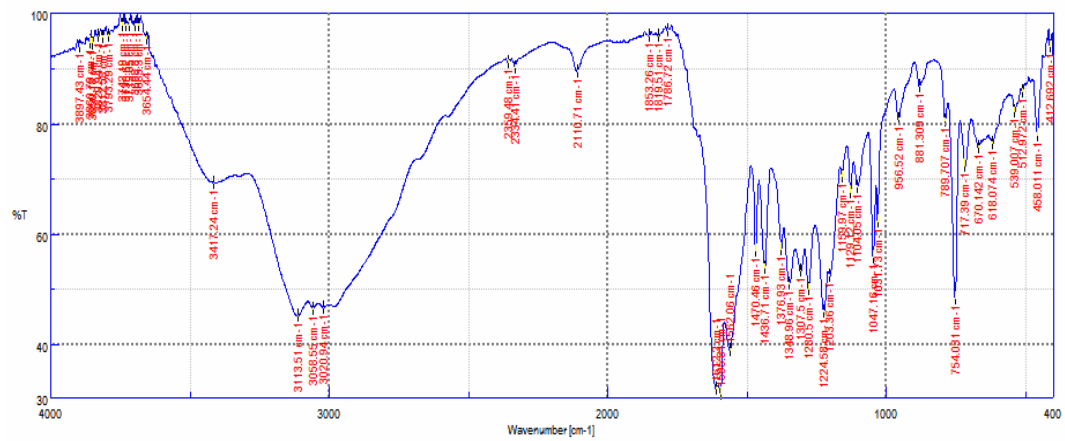


Fig.3.1B.iii The infrared spectrum of the platinum complex

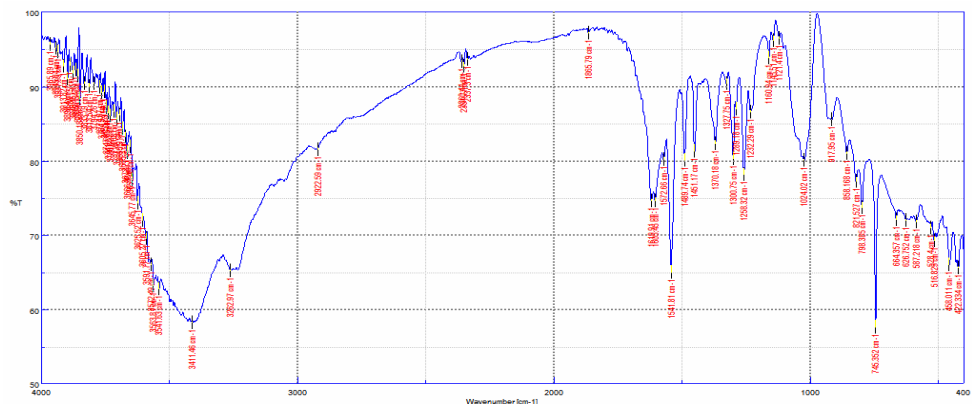


Fig.3.1C.i The infrared spectrum of the Schiff base (HEMTDT)

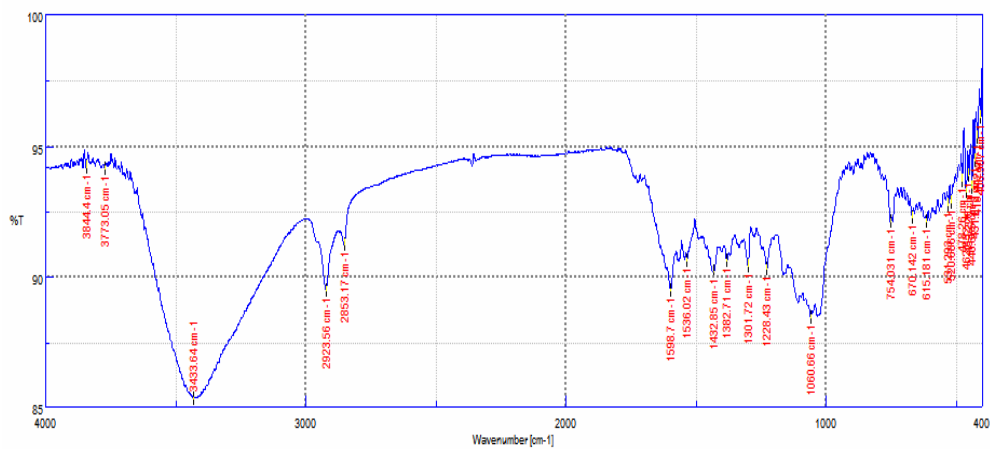


Fig.3.1C. ii The infrared spectrum of the cobalt complex

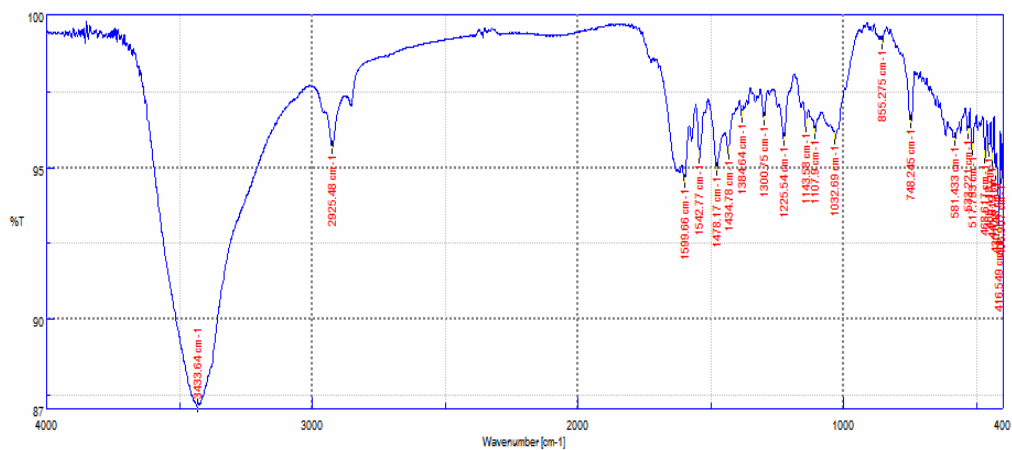


Fig. 3.1C. iii The infrared spectrum of the copper complex

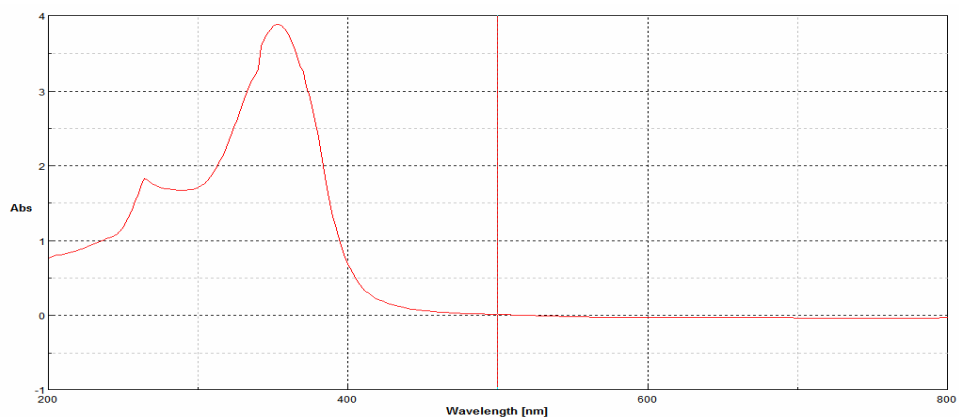


Fig. 3.2B. i The UV-visible spectrum of the cobalt complex

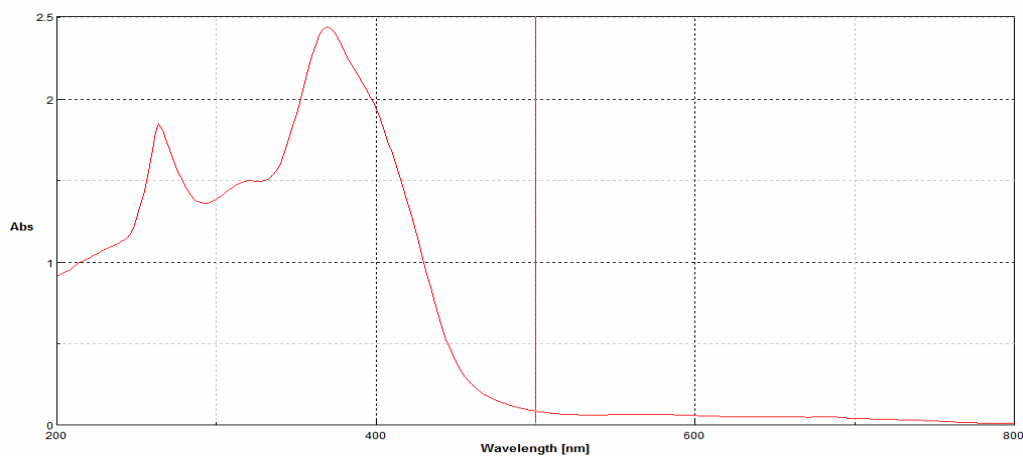


Fig. 3.2B .ii The UV-visible spectrum of the nickel complex

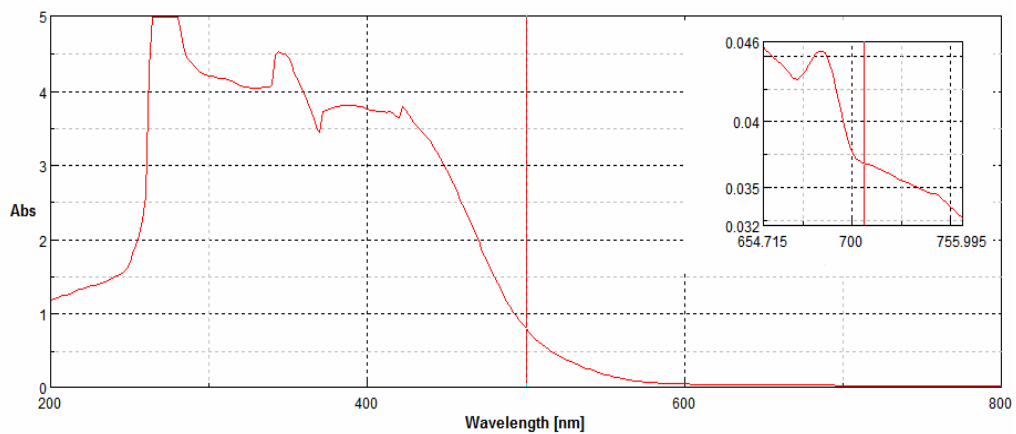
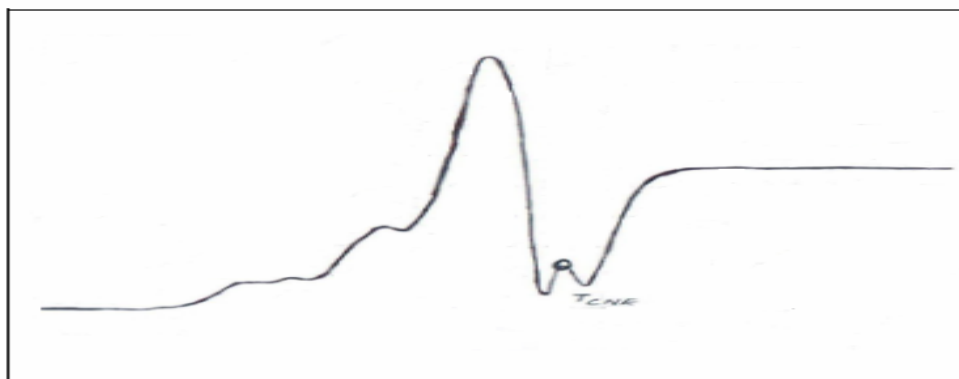
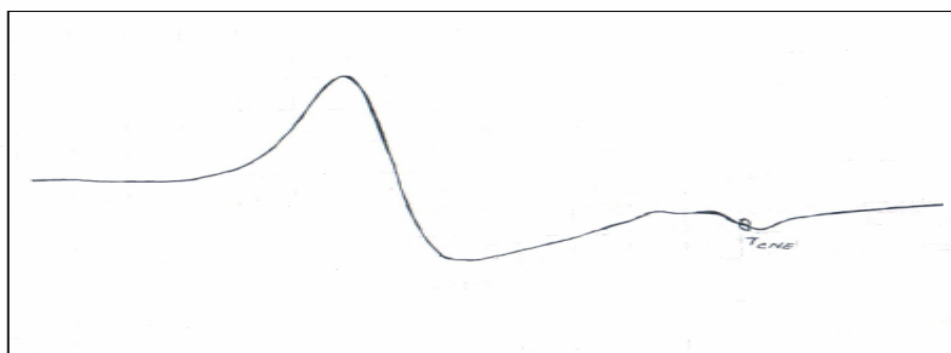


Fig. 3.2B. iii The UV-visible spectrum of the copper complex



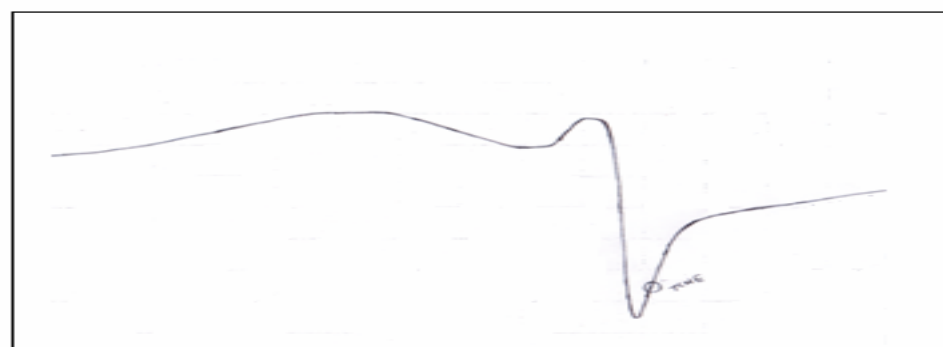
Field (G)

Fig.3.3A ESR spectrum of copper complex in solid state at room temperature



Field (G)

Fig.3.3B. ESR spectrum of copper complex in solid state at room temperature



Field (G)

Fig.3.3C . ESR spectrum of copper complex in solid state at room temperature

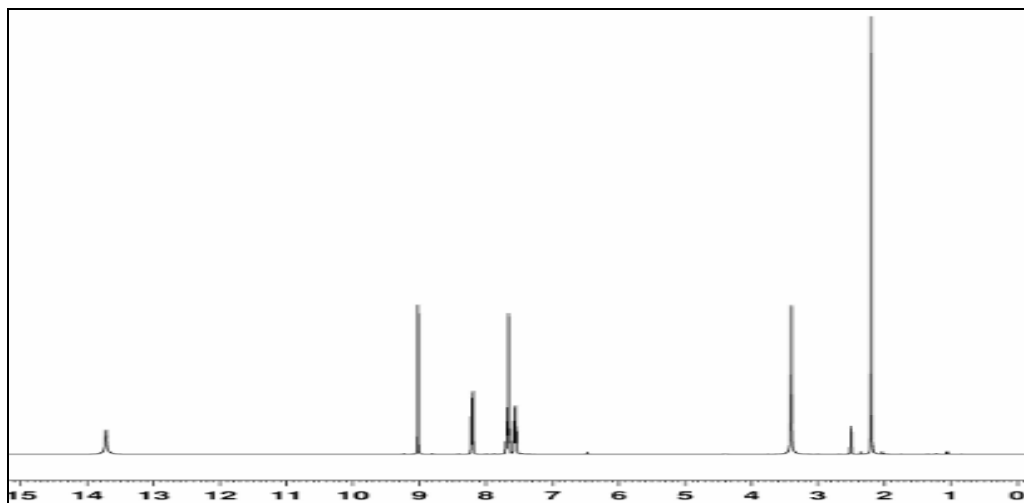


Fig. 3.4B .i. ^1H NMR spectrum of the ligand (CBMTDT)

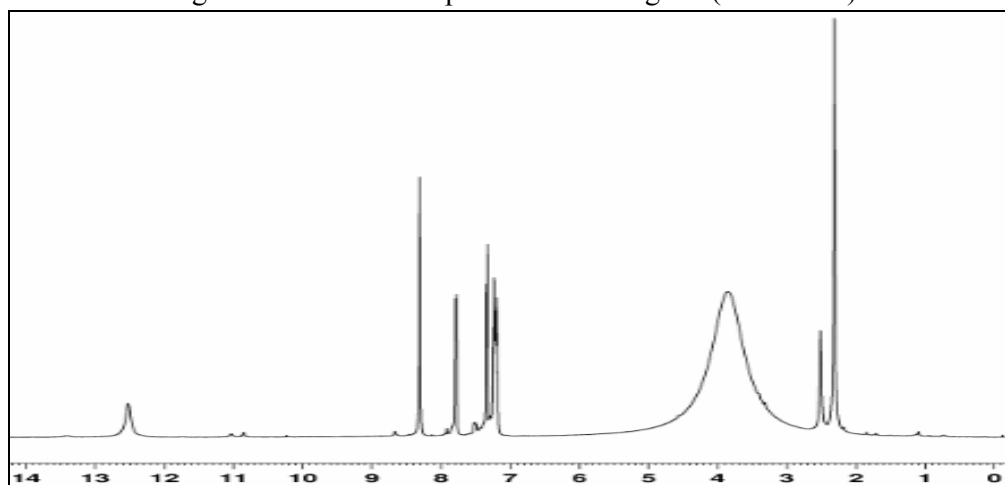


Fig.3.4B .ii ^1H NMR spectrum of the zinc complex

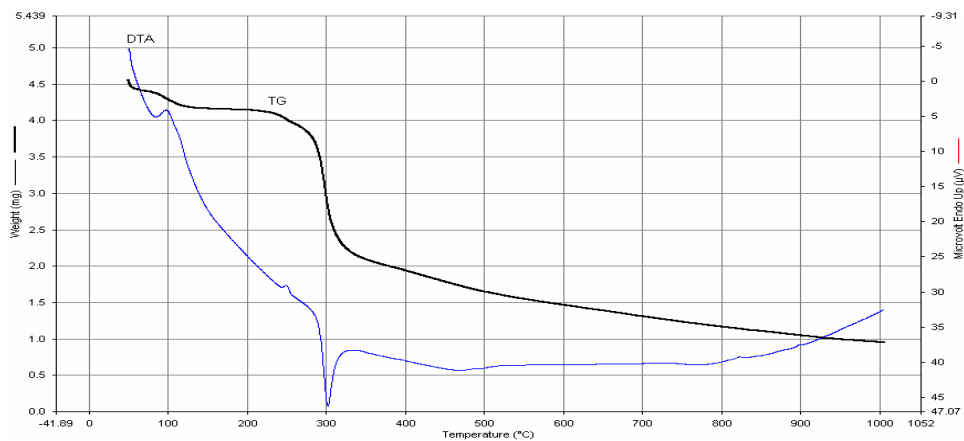


Fig.3. 5B iThe Thermogram of cobalt complex

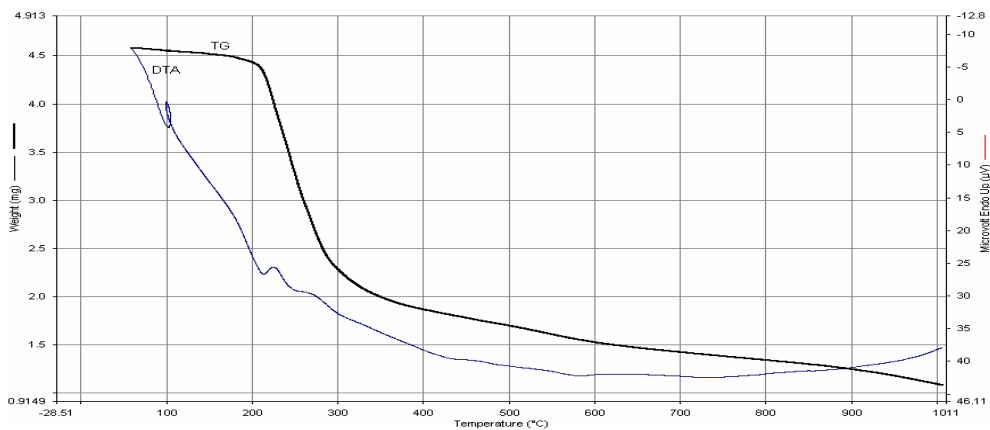


Fig.3.5B ii. Thermogram of zinc complex

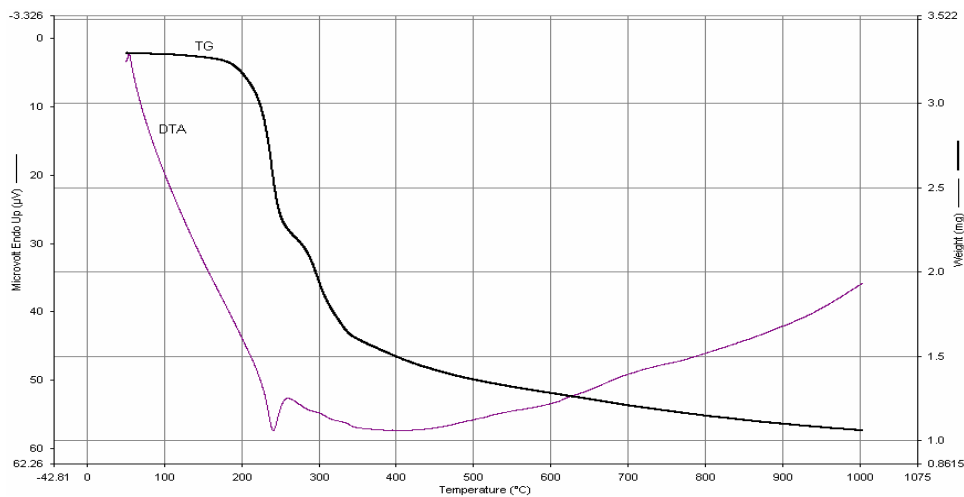


Fig.3.5B. iiiThermogram of copper complex

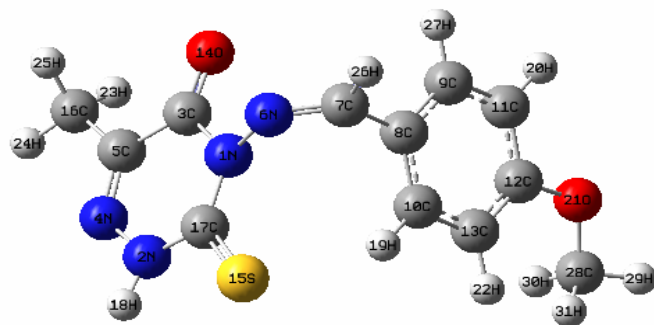


Fig. 3.6A Optimized geometry of the ligand(MMTDT)

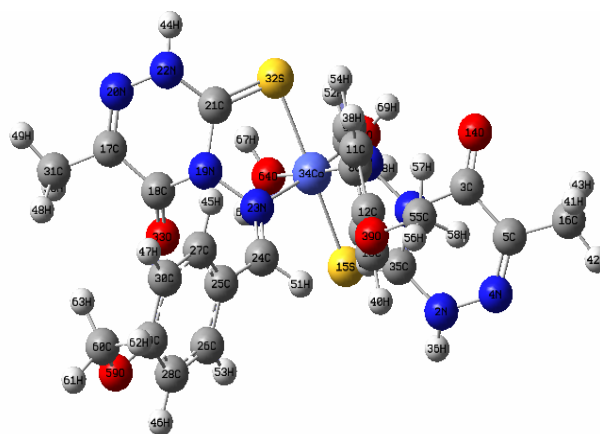


Fig. 3.7A .i Optimized geometry of the cobalt complex

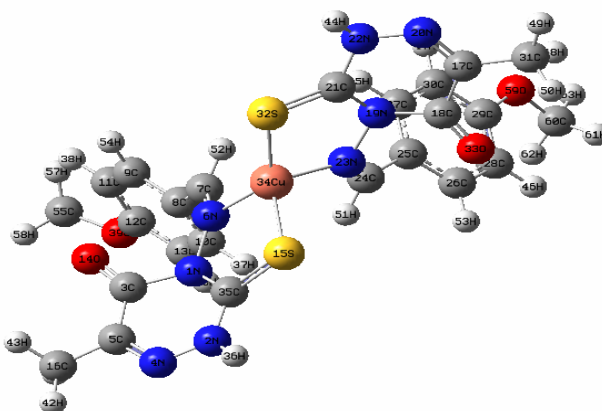


Fig. 3.7A. ii Optimized geometry of the copper complex

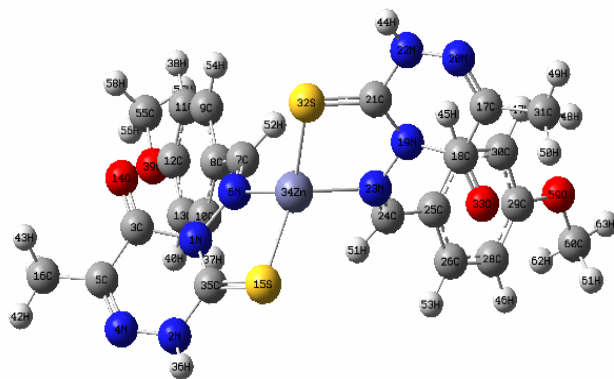


Fig. 3.7A. iii Optimized geometry of the zinc complex

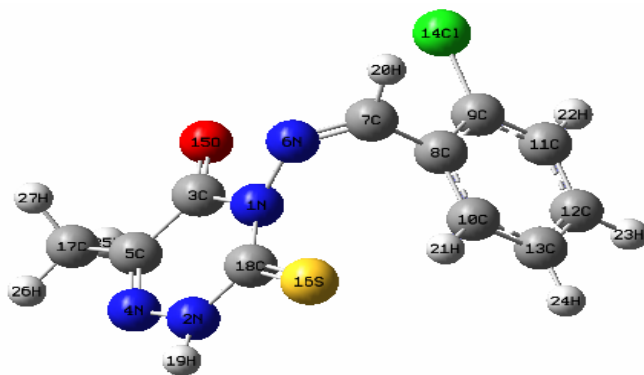


Fig. 3.6B Optimized geometry of the ligand (CBMTDT)

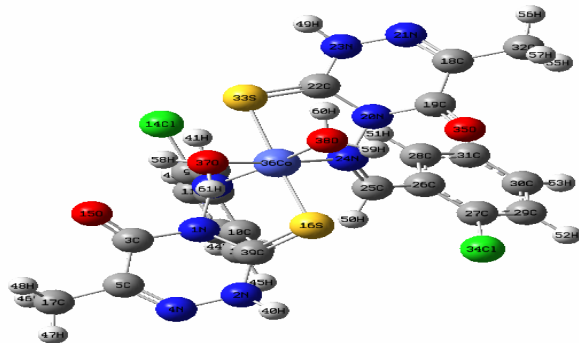


Fig.3.7B.i Optimized geometry of the cobalt complex

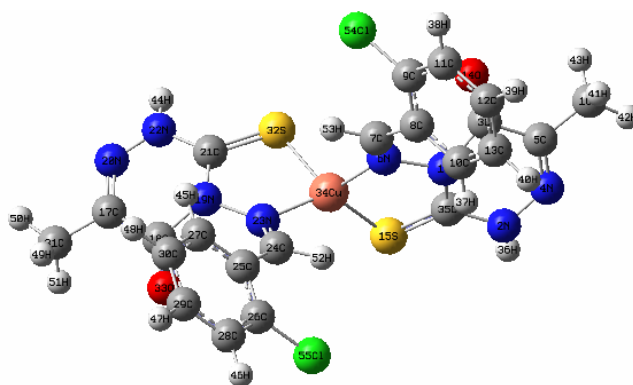


Fig.3.7B .iiOptimized geometry of the copper complex

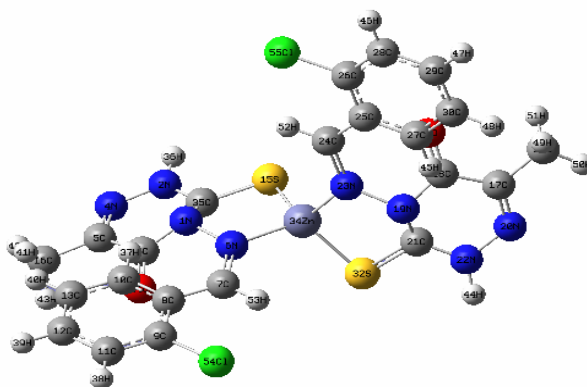


Fig.3.7B .iiiOptimized geometry of the zinc complex

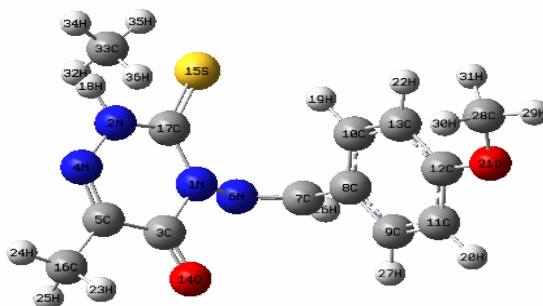
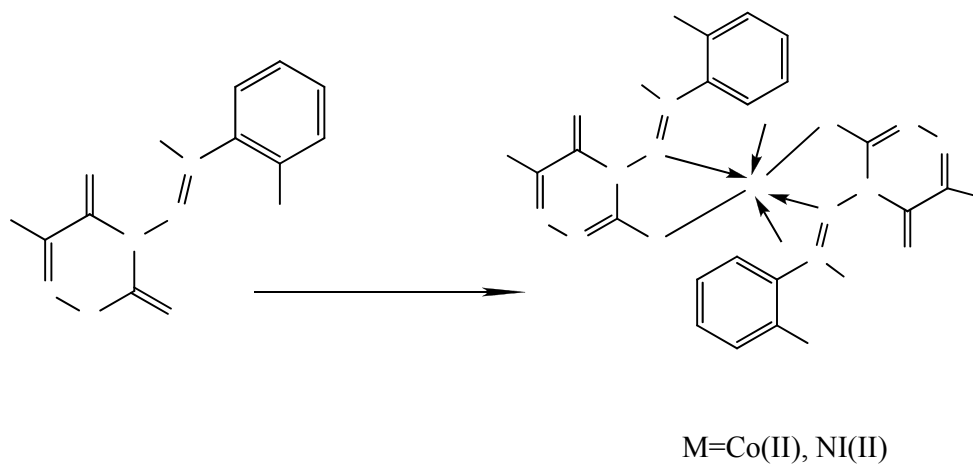
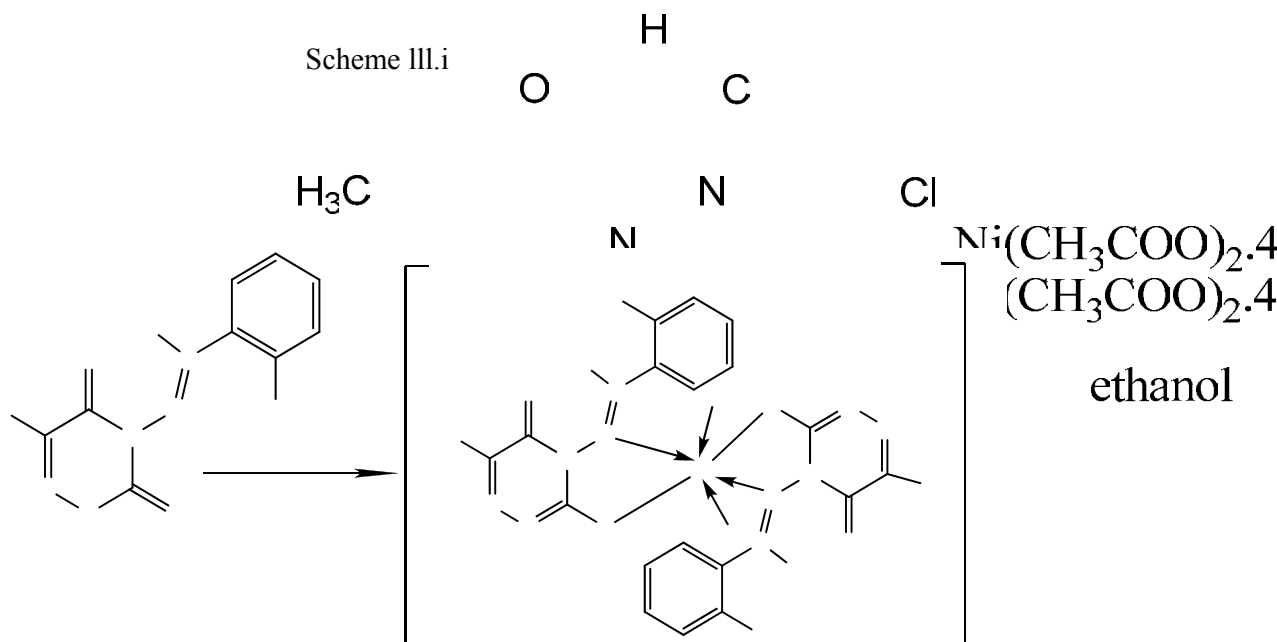


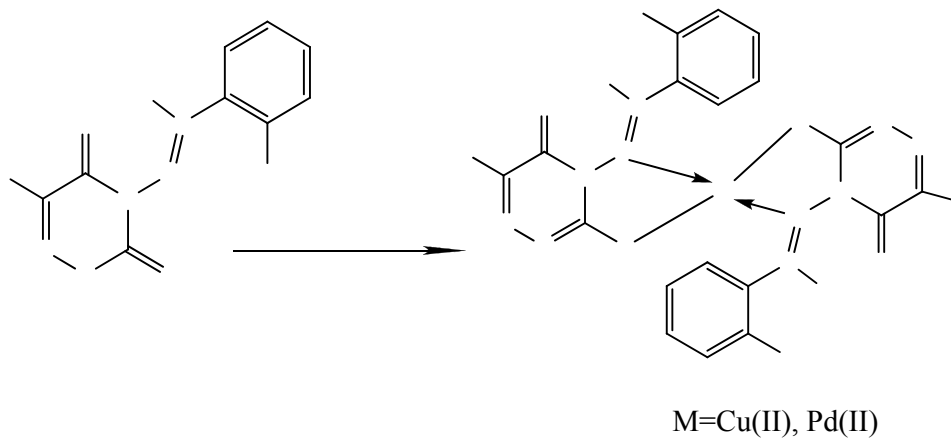
Fig.3.6C Optimized geometry of the ligand (HEMTDT)



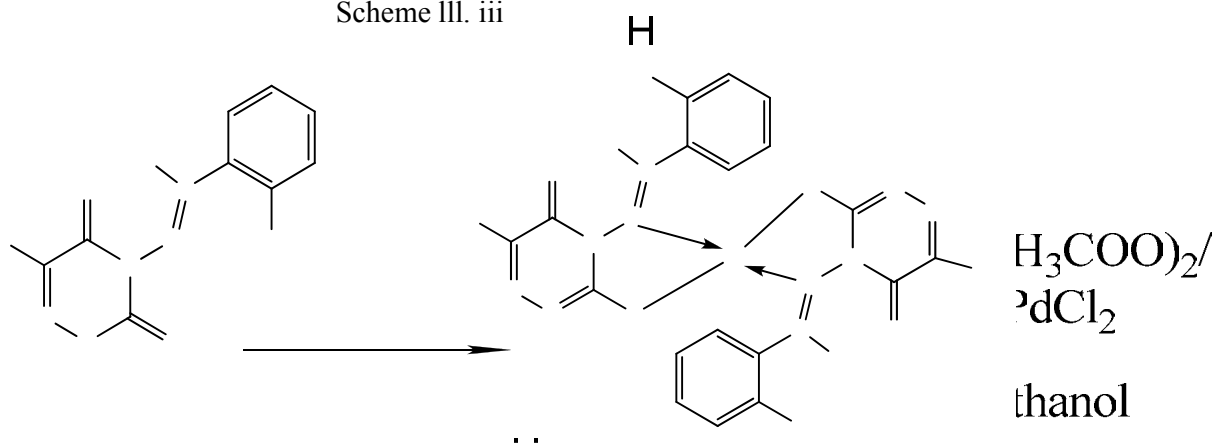
Scheme III.i



Scheme III.ii



Scheme III.iii



Scheme III.iv

